Durability Performance and Thermal Resistance of Structural Self-Compacting Concrete Improved with Waste Rubber and Silica Fume

Bušić, Robert; Miličević, Ivana; Dokšanović, Tihomir; Grubišić, Marin

buildings

MDPI

Article

Durability Performance and Thermal Resistance of Structural Self-Compacting Concrete Improved with Waste Rubber and Silica Fume

Robert Bušić *, Ivana Miličević, Tihomir Dokšanović and Marin Grubišić

Faculty of Civil Engineering and Architecture, Josip Juraj Strossmayer University of Osijek, 3 Vladimir Prelog Street, HR–31000 Osijek, Croatia; ivana.milicevic@gfos.hr (I.M.); tdoksanovic@gfos.hr (T.D.); marin.grubisic@gfos.hr (M.G.)

* Correspondence: rbusic@gfos.hr; Tel.: +385-97-699-76-95

Abstract: Waste rubber takes many years to decompose, and thus the increasing number of tires in the world can be characterised as an important environmental issue, which generated the idea of implementing crumb rubber in structural self-compacting concrete (SCC). According to previous studies, up to 15% recycled rubber and 5% silica fume can be used to achieve the required properties of SCC in reinforced structural members with congested reinforcement, both in the fresh and hardened state. Most studies have focused on investigating the mechanical properties of self-compacting rubberised concrete (SCRC), and only a small number of studies investigated the durability and thermal properties, with contradictory findings. This study aims to determine the influence of crumb rubber and silica fume on the durability and thermal properties of SCC, with an emphasis on the selection of environmental exposure classes, the safety of using such a material in reinforced concrete members, and additional serviceability and durability requirements. This was further advanced by investigating the micro-structure of hardened SCC with recycled rubber and silica fume using a scanning electron microscope (SEM). Test results indicate that the combining effect of crumb rubber and silica fume has a positive impact on the thermal and durability properties of SCC.

Keywords: sustainability; supplementary cementitious materials; waste tires; green materials; optimal mixture; micro-structural analysis

Citation: Bušić, R.; Miličević, I.; Dokšanović, T.; Grubišić, M. Durability Performance and Thermal Resistance of Structural Self-Compacting Concrete Improved with Waste Rubber and Silica Fume. *Buildings* **2023**, *13*, 1331. https://doi.org/10.3390/buildings13051331

Academic Editors: Haleh Rasekh and Marie Joshua Tapas

Received: 28 April 2023
Revised: 12 May 2023
Accepted: 16 May 2023
Published: 19 May 2023

1. Introduction

The fact that approximately 70% of the mass of concrete is made of fine and coarse aggregates is an opportunity for a thorough study of the impact of using recycled rubber as an alternative material to natural aggregates. Such a use case can lower concrete weight and conserve natural resources, but also potentially improve certain properties of concrete. Natural aggregate is used as a component of asphalt and concrete and is required for the construction of almost every part of the built environment, such as roads, railroads, bridges, buildings, pavements, sewers, dams, etc. Globally, aggregate is a leading mineral commodity in terms of quantity and quality. In 1998, about 20 billion metric tons of aggregates worth 120 billion euros were produced [1]. The demand for aggregates as raw materials increases by 4.7% every year [2], which would mean that the consumption of natural aggregates in 2022 is more than 50 billion metric tons per year. According to [3], if only 10% of natural aggregates were replaced by recycled rubber, the consumption of natural aggregates would decrease by approximately 4.83 billion metric tons per year. One of the main directions of research on SCC is to improve its properties while making the material more environmentally friendly and sustainable, both by reducing the number of waste car tires in landfills and reducing the use of natural aggregates as a limited resource. Recycled rubber has a slightly higher market value than natural small aggregates, but with a faster expansion of the green economy, promotion of recycled materials, and improvements

in processing and treatment of waste tires, a reduction in price and positive effects of using recycled rubber as a component in concrete mixtures can be expected in the near future.

Scientists and engineers have been testing the physical–mechanical and dynamic properties of ordinary and self-compacting rubberised concrete for many years. The general conclusions are as follows, the addition of rubber to concrete decreases density [4–7], compressive strength [4,5,8–10], and modulus of elasticity [5,9–12], and increases porosity [5,13,14], impact resistance [7,13,15–17] and ductility [9,17–19]. There are plenty of studies published concerning the durability [20–28] and thermal properties [28–35] of conventional concrete with recycled rubber, but research results on these properties are inconsistent. Moreover, only a small number of authors have studied the durability and thermal properties of SCRC. Si et al. [12] investigated SCC with 15 and 25% rubber content with the addition of fly ash. They concluded that as the rubber content increased, the shrinkage of the concrete also increased. However, Zaoiai et al. [6] partially replaced natural fine and coarse aggregate with rubber aggregate (size 0/3 and 3/8) in various amounts and reported a reduction in 28-, 90-, 200-, and 300-day shrinkage with an increase in rubber aggregate content. There is a lack of experimental studies on the water and gas permeability of SCRC, and there is no question that this durability property of SCRC should be investigated. Only Jedidi et al. [36] studied the thermal conductivity of SCRC, where they partially replaced natural gravel in SCC mixtures with rubber aggregates (size 0/4 and 4/8), in different amounts (0%, 10%, 20%, and 30%). They reported a reduction in thermal conductivity from 1.3 to 0.76 W/mK, a reduction of 41.5% for an increase in rubber content from 0% to 30%. Regarding the freeze–thaw resistance of SCRC, Topçu and Bilir [37] reported a reduction in the compressive strength of SCC specimens in which fine aggregate was replaced with rubber (size 0–4 mm) at different mass percentages of 60, 120, and 180 kg/m^3—9.34%, 15.25%, 28.15%, and 28.47%, respectively. The same authors [37] investigated the resistance of SCRC to high temperatures (400 °C and 800 °C), and they again reported a reduction in the compressive strength for specimens in which fine aggregate was partially replaced by rubber (size 0–4 mm). Previous studies of SCRC [38–41] concluded that up to 15% recycled rubber and 5% silica fume can be used to achieve the required properties of SCC, both in the fresh and hardened state, suitable for structural members with densely distributed reinforcement. However, as the literature review indicates, consistent experimental work regarding the effects of waste tire rubber on the durability and thermal properties of SCC is needed.

The properties of self-compacting rubberized concrete (SCRC) can vary depending on various factors such as mixture design, material properties, and the type and size of recycled rubber used. Using CR as a replacement for natural fine aggregate can have negative effects on the fresh and hardened state properties of SCC. Therefore, mineral and chemical additives, such as different types of supplementary cementitious materials (SCMs) and superplasticizers, are necessary to maintain the desired properties of the concrete. The negative impact of rubber on the mechanical properties of self-compacting concrete can be neutralized or reduced by adding various types of mineral additives to the concrete. The use of mineral additives can significantly improve the mechanical properties of self-compacting concrete [42,43]. Several studies have investigated the individual and mutual effects of SLF and other SCMs, including fly ash, metakaolin (MK), and ground granulated blast-furnace slag (GGBFS), on the properties of highly flowable cementitious composites [44–46] while other studies investigated the individual effect of SLF on SCC properties [47–49]. Due to its small spherical particle shape, silica fume provides good cohesion and improved resistance to segregation, successfully eliminating water segregation and separation [50], which potentially makes it the most suitable cement additive in the observed case. The very small particles of silica fume, which are about 10 times smaller than cement particles, and the large specific surface area of silica fume contribute to the increase in the volume surrounding cement particles. Furthermore, silica fume increases reactivity, accelerates hydration, and reacts with free lime, creating calcium-silicate hydrate (C-S-H) gel [51]. Wang et al. [43] conducted a study to examine how the combination

of silica fume and fly ash affects drying shrinkage in concrete. Their findings indicate that utilizing both silica fume and fly ash can result in a decrease in drying shrinkage. Increasing the amount of silica fume in concrete also increases the compressive strength values of concrete [43] and thus its brittleness, which, in the case of rubber concrete, which has increased ductility [9] and deformability capacity [52], is not a problem, but a desirable occurrence. The combined effect of silica fume and recycled rubber potentially results in concrete with maintained initial mechanical properties, as well as increased deformability and ductility. Since it is desirable in some applications for concrete to have a lower density, high ductility, and energy absorption capacity, the combination of rubber granules and silica fume can contribute to the development of innovative concrete with increased ductility and flexibility, as well as potentially good thermal properties.

The main objective of this study is to conduct additional research on SCC with recycled rubber and silica fume at the material level, especially regarding durability and thermal properties. Additional aims include testing the microstructure of hardened SCC with recycled rubber and silica fume using a scanning electron microscope (SEM), with particular emphasis on the selection of environmental exposure classes, the safety of using such a material in reinforced concrete members, and additional serviceability and durability requirements. The purpose of the study is consequently to provide insight into important parameters of SCRC, which are currently missing when forming an integral assessment of this material and its potential for use in civil engineering.

2. Experimental Program

2.1. Materials and Mixture Design

Materials used in this experiment were adopted from the authors' previous work [41], as well as three SCC mixture designs that were defined as optimal for future studies of SCC with CR (Table 1). Mixtures with constant water-to-cement ratio (w/c) of 0.4 by weight were produced. To increase flowability, superplasticizer (SP) Energy FM500 was used. Portland cement type CEM I 42.5R was used, with a density of 3.17 g/cm^3. To increase the segregation resistance of several SCC mixtures, a viscosity-modifying admixture (VMA) was added. An 80 kg/m^3 of dolomite powder with a density of 2.97 g/cm^3 was used as a filler in each SCC mixture. Silica fume (SLF), with a specific gravity of 2.2 g/cm^3 and Blaine fineness of 20.5 m^2/g, was used as a supplementary cementitious material (SCM). The density of naturally fine and coarse aggregate was 2.58, 2.79, 2.88 and 2.88 g/cm^3 for fractions 0–2, 0–4, 4–8 and 8–16 mm, respectively. Recycled crumb rubber, obtained by mechanically grinding local waste tires, with grain size 0–4 mm and density of 1.05 g/cm^3, was used as a replacement material for natural fine aggregate. The reference SCC mixture SCC-R and mixtures with 10 and 15% of CR and 0 and 5% of silica fume (SLF) (SCC-10-0 and SCC-15-5) were designed according to the European guidelines for SCC [53]. In a previous study [41] it was observed that the slump flow class was changed from SF3 to SF2 and SF1 when the proportion of CR was increased from 0 to 10 and 15%, respectively. Since the slump flow class, SF3 is widely used in concrete members with congested reinforcement, the amount of superplasticizer (SP) was not kept constant in this study. In addition, the segregation resistance can be decreased with the addition of SP. Therefore, a viscosity-modifying admixture (VMA) was added to the SCC mixture without SLF to prevent bleeding.

Table 1. Proportion of self-compacting concrete mixtures (kg/m^3).

No.	Mixture ID	Cement	SLF	VMA	Crumb Rubber	Natural Aggregate (Dolomite)			
					0–4 mm	0–2 mm	0–4 mm	4–8 mm	8–16 mm
1	SCC-0-0	450	0	1.08	0	325.54	616.07	363.40	454.25
2	SCC-10-0	450	0	1.08	66.24	325.54	439.30	363.40	454.25
3	SCC-15-5	427.5	22.5	0	98.91	324.04	350.42	361.72	452.15

2.2. Mixing, Casting, Curing Conditions and Test Methods

A pan mixer with a capacity of 50 L was used, utilising a mixing procedure adopted from a previous experiment [41]. Immediately after mixing, the properties of the fresh SCC were investigated. The fresh state properties of SCC mixtures were in accordance with relevant European standards [54–57]. The concrete was cast into standardised moulds without vibration or compaction. Mechanical properties were determined 28 days after casting and water curing. Compressive strength and modulus of elasticity were determined on cylindrical specimens (Ø150 × 300 mm), while flexural strength was determined on prisms (100 × 100 × 400 mm). The mechanical properties were determined according to relevant European standards [58–60]. Gas permeability was tested according to the CemBureau method recommended by RILEM TC 116-PCD [61] on nine Ø150 × 50 mm specimens of each SCC mixture, prepared by cutting from three Ø150 × 300 mm cylinder specimens. The specimens were dried in an oven at 105 °C until a constant weight was achieved. The water penetration depth under pressure was tested according to EN 12390-8 [62] using a Controls 55-C0246/6 measuring device. The test was performed on two series of three specimens each, i.e., six specimens from each SCC mixture investigated. Drying shrinkage tests were performed according to EN 12390-16 [63]. Three prisms (dimensions 100 × 100 × 400 mm) were prepared from each SCC mixture. The specimens were removed from the moulds 24 h after casting. After de-moulding, the specimens were stored in a chamber at a temperature of 20 ± 4 °C and relative humidity of 70 ± 5%. The length change was measured with a length comparator every 7 days up to 91 days of age. Freeze–thaw resistance was tested according to CEN/TS 12390-9 [64]. Concrete specimens of 150 × 150 × 50 mm were previously prepared at 21 days of age by sawing cubic specimens. After 28 days of water curing, four specimens were prepared from each SCC mixture, placed in an air-conditioned chamber, and subjected to 56 freeze–thaw cycles. After 7, 14, 28, 42, and 56 cycles, the mass of the dried scaled material of the test surface was determined.

The mechanical properties (compressive strength, stress–strain relation, and modulus of elasticity) of cylindrical SCC specimens Ø150 × 300 mm exposed to high temperatures (0, 200, 400, 600, 800 °C) were determined according to RILEM TC 200-HTC [65] and EN 12390-13 [60]. The SCC specimens were de-moulded 24 h after casting and placed in a water tank. At 28 days of age, the specimens were removed from the water tank and stored at a laboratory room temperature of 20 ± 2 °C and a relative humidity of 30 ± 5%. At one year of age, the specimens were dried in an oven at 105 °C until the weight change was less than 0.1% and then they were exposed to high temperatures. According to the RILEM recommendations [65] and the diameter of the cylindrical SCC specimens, a constant value of the heating rate of 0.5 °C/min was adopted. Thirty cylindrical SCC specimens were prepared from each SCC mixture, six specimens for each of the test temperatures (0, 200, 400, 600, 800 °C). The specimen temperature change was monitored at the specimen surface and centre with K-type thermocouples while the furnace temperature change was monitored with a probe. The applied heating and cooling rates are shown in Figure 1, with introduced intervals at maximum temperatures shown in Figure 2. Upon completion of the heating process, the specimens were left in the furnace until reaching room temperature. In addition to the mechanical properties already mentioned, various other parameters were observed and studied: change in mass and colour, ultrasonic pulse velocity (UPV), explosive spalling, crack development, and microstructural changes by using a scanning electron microscope (SEM).

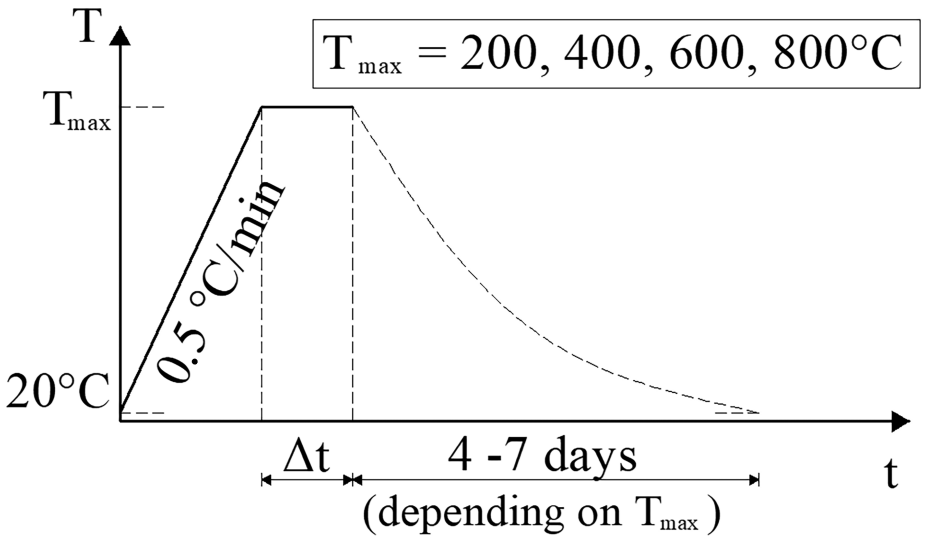

Figure 1. Heating and cooling rates of SCC specimens.

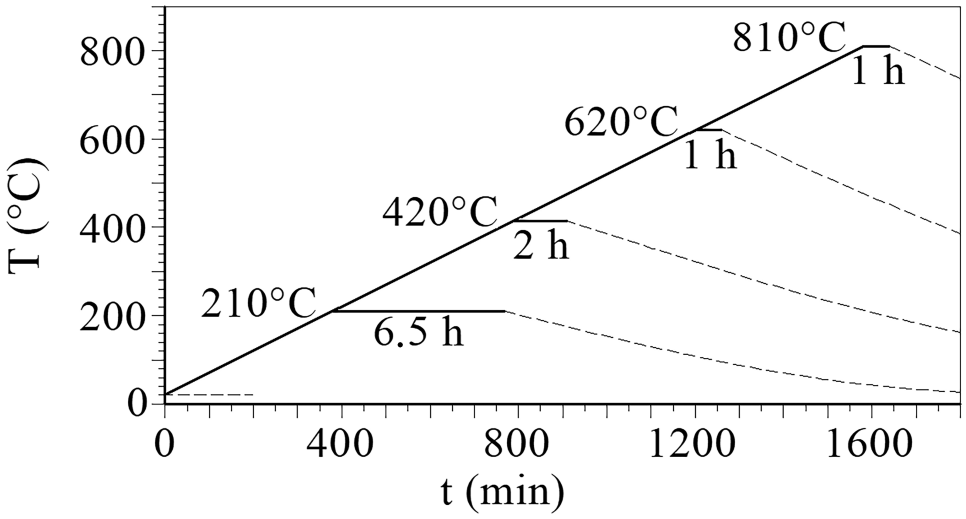

Figure 2. The heating regime of SCC specimens.

Thermal conductivity for all mixtures was determined on cylindrical specimens with a diameter of Ø150 mm, following EN 12667 [66] and ISO 8302 [67]. The measuring was performed using an FOX200 instrument with external thermocouples. Before testing, specimens were dried in the oven at 105 °C until a constant weight was reached. Four specimens of each SCC mixture were tested.

3. Experimental Results and Discussions

3.1. Fresh State Properties

The test results for the fresh SCC properties are presented in Table 2, and as expected they coincide with those presented in [41]. The sieve segregation test was performed as needed after visually inspecting the fresh concrete paste. Segregation was not observed in mixture SCC-15-5; therefore, the sieve segregation test was not conducted for this mixture. Crumb rubber negatively affects flowability and passing ability, reduces segregation resistance and increases viscosity. To counteract these effects, the amount of SP was increased from 1.25 % to 1.5 %, which reduced the negative effect of the rough surface and sharp edges of CR.

Table 2. Test results of fresh SCC properties.

Mixture	Flowability		Viscosity		Passing Ability				Segregation Resistance	
	Slump Flow		T500		J-Ring		L-Box		Sieve Segregation	
	d (mm)	Class	(s)	Class	PJ (mm)		(H_2/H_1)	Class	%	Class
SCC-R	770	SF3	1.83	VS1	10	≤ 10	0.97	> 0.80	10.22	SR2
SCC-10-0	760	SF3	1.75	VS1	11	> 10	0.95	> 0.80	8.11	SR2
SCC-15-5	655	SF2	1.91	VS1	18	> 10	0.91	> 0.80	—	SR2

3.2. Mechanical Properties

The testing of the mechanical properties of SCC is not the main focus of this paper. However, to obtain an additional validation of mixtures per results in [41], compressive strength ($f_{c,cyl}$), modulus of elasticity (E), and flexural strength (f_b) were investigated. Test results of these mechanical SCC properties are presented in Table 3. The results validate that the mixtures achieved mechanical properties that match those presented in [41].

Table 3. Test results of mechanical SCC properties.

Mixture	$f_{c,cyl}$ (MPa)			E (GPa)			f_b (MPa)		
	Mean	St. Dev. [1]	CoV% [2]	Mean	St. Dev. [1]	CoV% [2]	Mean	St. Dev. [1]	CoV% [2]
SCC-R	48.24	1.99	4.12%	38.25	2.35	6.13	7.30	0.42	5.72%
SCC-10-0	29.21	0.77	2.64%	29.82	1.45	4.86	6.85	0.24	3.54%
SCC-15-5	29.07	1.01	3.48%	24.76	0.61	2.45	5.90	0.32	5.39%

[1] Standard Deviation. [2] Coefficient of Variation.

3.3. Durability and Thermal Properties

3.3.1. Gas Permeability

The test results for the gas permeability coefficient are presented in Table 4. The increase in gas permeability of SCC with increased content of recycled rubber can be explained by the rough surface and sharp edges of the rubber, which retains air in the structure of test specimens, increasing the porosity of SCC and consequently gas permeability. The increase can also be attributed to the fact that recycled rubber deforms under gas pressure, easily finding its way through the specimen [20]. The gas permeability did not significantly increase with the increase in rubber content from 10% to 15%, as was previously reported by Guneyisi et al. [21] and explained by the improved pore structure in the concrete as a result of the contribution of silica fume. According to the criteria for determining the quality of concrete concerning the values of the gas permeability coefficient [68], all three concrete mixtures are considered medium-quality concrete. Regarding gas permeability and according to the classification given by the RILEM recommendations [68], it can be concluded that SCC with 10% and 15% recycled rubber content can be used in structural reinforced concrete members without additional restrictions.

Table 4. Mean values of gas permeability coefficient (in m^2) and depth of penetration of water under pressure (in mm).

Mixture	Gas Permeability Coefficient (m^2)	Depth of Penetration of Water under Pressure (mm)	
		Series 1	Series 2
SCC-R	1.41×10^{-16}	18.41	18.75
SCC-10-0	1.86×10^{-16}	33.58	34.68
SCC-15-5	2.37×10^{-16}	34.50	34.33

3.3.2. Water Permeability

The test results for the depth of penetration of water under pressure are given in Table 4. The reference mixture SCC-R has the lowest mean value of the water penetration depth and according to HRN 1128 [69] it can be classified as VDP2. Concrete mixtures SCC-10-0 and SCC-15-5 have approximately the same average value of water penetration depth and according to HRN 1128 [69] can be classified as VDP3. The depth of water penetration increases with the addition of recycled rubber, which is in agreement with previous research [22,23]. This behaviour can be explained by the decrease in capillary absorbency when recycled rubber [23] as a non-waterproof and hydrophobic material was implemented, increasing the water permeability in the contact area of "recycled rubber–cement paste" due to entrapped air and weak interfacial transition zones. Furthermore, the average value of the depth of water penetration of concrete mixtures with 10% and 15% of recycled rubber was very similar (between 33–35 mm). Increasing the percentage of rubber replacement from 10% to 15% would certainly have an impact on increasing the depth of water penetration, but this type of occurrence was prevented by the addition of silica fume, which positively affects the bond between recycled rubber and cement paste [22]. A similar positive effect of silica fume on concrete mixtures with recycled rubber was described in the previous chapter where the gas permeability of concrete mixtures with 10% and 15% rubber were quite similar. Both of these findings lead to the conclusion that the test results of these two durability properties are correlated. Based on the test results of water permeability, it is recommended to limit the use of SCC with 10% and 15% recycled rubber to situations where the material is not exposed to direct contact with pressurised water.

3.3.3. Drying Shrinkage

The drying shrinkage of investigated SCC mixtures is presented in Figure 3. The values presented are the mean values of three prisms. After 7 days, the mean drying shrinkage of SCC-R is 43% higher and 9% lower compared to the mean drying shrinkage of SCC-10-0 and SCC-15-5, respectively. Furthermore, the SCC-15-5 mixture shows the highest mean values of drying shrinkage, which can be explained by the higher fineness of silica fume compared to cement. As the shrinkage of concrete causes stresses, cracks occur, meaning that the process of concrete shrinkage is an unfavourable occurrence in terms of concrete serviceability. Therefore, the value of the concrete shrinkage must be as low as possible, especially in the first days after concreting, indicating that the SCC-10-0 mixture is the best in these terms (36% lower average drying shrinkage after 7 days, compared to the SCC-15-5 mixture). Between the 14th and 91st day, reference SCC mixture SCC-R has the highest value of drying shrinkage compared to mixtures SCC-10-0 and SCC-15-5, up to 45% and 27%, respectively, which is in line with test results reported by [6], but also in contradiction with some of the test results reported in [5,12]. The reduced drying shrinkage of mixtures with waste rubber can be explained by increased deformability, mostly since recycled rubber is more elastic than natural aggregate and it does not bind water molecules to itself. It can be concluded that replacing natural aggregate with recycled rubber has a positive effect on drying shrinkage. Recycled rubber contributes to the potential reduction in the number and size of cracks in SCC specimens, which consequently provides higher durability and lower maintenance costs of concrete during the design life of the building. The drying shrinkage of investigated SCC mixtures can be predicted with high accuracy ($R^2 > 0.9$) using logarithmic regression equations based on Figure 3:

$$\text{SCC-R} \qquad y = -0.129 \cdot \ln(x) + 0.056 \tag{1}$$

$$\text{SCC-10-0} \qquad y = -0.106 \cdot \ln(x) + 0.06 \tag{2}$$

$$\text{SCC-15-5} \qquad y = -0.099 \cdot \ln(x) + 0.0197 \tag{3}$$

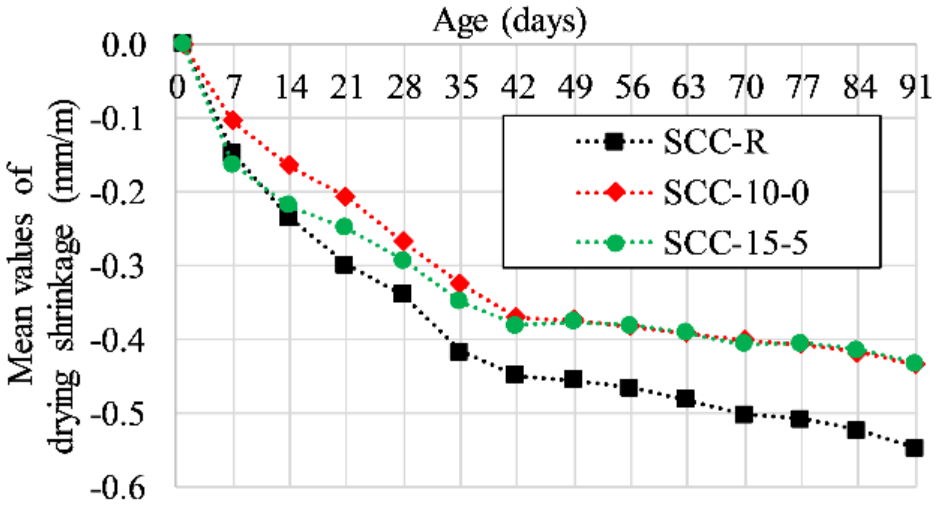

Figure 3. Drying shrinkage of SCC prisms.

3.3.4. Freeze–Thaw Resistance

The mean values of the mass of scaled material after 56 freeze–thaw cycles (S_n) are presented in Figure 4. For all observed cycles, the mean values of the mass of scaled material were the highest for the reference SCC mixture and lowest for the SCC-10-0 mixture. Furthermore, with 15% recycled rubber, the mass of the scaled material after 7, 14, 28, 42, and 56 freeze–thaw cycles was smaller compared to the mass of the scaled material of the reference SCC mixture. After 7 and 14 freeze–thaw cycles, the difference between the mean values of the mass of scaled material was less visible. After 28 freeze–thaw cycles there was a significant increase in this difference, most pronounced after 56 freeze–thaw cycles, where the mass of the scaled material of the mixture SCC-R was 10 and 3 times higher than the mass of scaled material of mixtures SCC-10-0 and SCC-15-5, respectively. To date, several studies on freeze–thaw resistance of traditional concrete with rubber have been carried out with similar test results [22,24–26]. However, the results of several studies have shown the opposite [26,27], at least in terms of a higher percentage of replacement of natural aggregate with rubber. Liu et al. [26] concluded that the positive effect of rubber on the concrete freeze–thaw resistance is expressed only up to 5% replacement of natural aggregate with recycled rubber, which is not the case in this study where better resistance to freeze–thaw cycles was achieved with higher replacement levels.

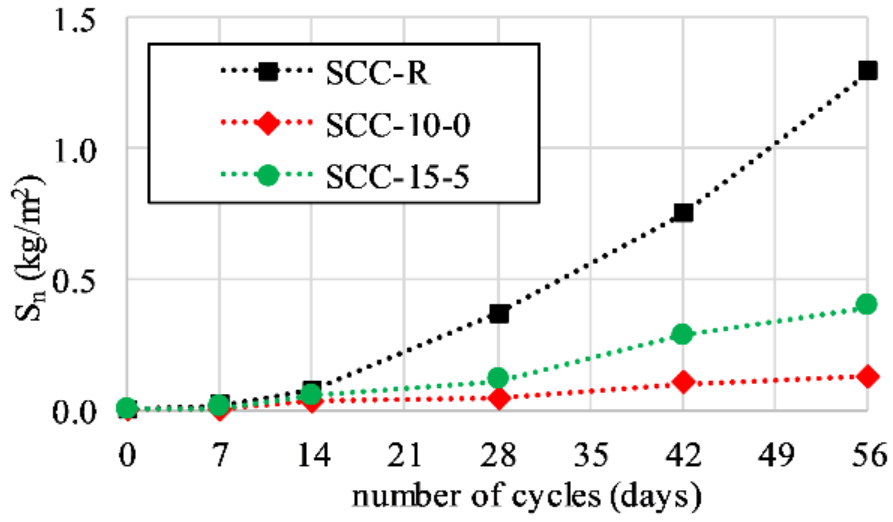

Figure 4. Mass of scaled material after 7, 14, 28, 42, and 56 freeze–thaw cycles (S_n).

In previous research [25,28], it was concluded that the grain size of the rubber plays an important role in the scaling of concrete after freeze–thaw cycles. The best results were obtained when the fine rubber aggregate was used, as it has a larger specific surface area compared to coarse recycled rubber, causing an increased number of micropores that entrap air in cement paste. The air increases the porosity of the concrete mixture and provides a higher resistance to freeze–thaw cycles, similar to the effects provided by the use of aerants [70]. Furthermore, the rough edges of rubber entrap air bubbles, which provides better transmission of the internal stresses caused by an increase in volume due to the transition of water from liquid to solid state. Internal forces which occur during expansion in concrete with recycled rubber have less destructive consequences as the higher amount of micropores provides additional space for ice and salt crystals [24] to spread at temperatures below 0 °C. The rubber itself is more resistant to freezing than natural aggregate and can provide a mechanism in which through greater deformability it absorbs internal stresses caused by an increase in volume, thus relieving stress from the surrounding cement paste. The described mechanism also prevents the premature occurrence of cracks in concrete, which is associated with an improvement in the serviceability of the concrete. It is important to point out that recycled rubber can not only be used as a substitute for natural aggregate but also as an aerant, providing savings for concrete intended for use in an environment where there is a risk of corrosion caused by freeze–thaw cycles.

According to the test results, SCRC can also be used in structural members in areas where the concrete structure is exposed to freezing and thawing, in contact with de-icing salts (e.g., where water spraying from traffic areas occurs). According to HRN 1128 [69] and EN 206 [71], test results meet the condition for the usage of SCC with 10 and 15% of recycled rubber in conditions where exposure classes XF2 or XF4 are required. This leads to the general conclusion that recycled rubber has a positive influence on the resistance of SCC to freeze–thaw cycles.

3.3.5. Resistance to High Temperatures

Similar to the conclusion of the experiment conducted by Hernandez-Olivares and Barluenga [72], concrete specimens without recycled rubber showed a greater spalling effect compared to concrete specimens with recycled rubber. Reduction in spalling can be explained by the occurrence of voids formed in the places of burnt recycled rubber located near the surface of the concrete specimens, which consequently lead to a reduction in internal compressive stresses caused by gases and water vapour. The surface structure of concrete is thus preserved, which can improve the durability of concrete and reinforcement in the form of a reduced number of cracks, preservation of the protective layer, and thus better protection of reinforcement in structural members during exposure to high temperatures or fire.

After exposure to high temperatures, the occurrence of cracks is typical for reference SCC specimens at 400, 600, and 800 °C. After exposure to 400 and 600 °C, cracks appeared at the bottom of the specimen (Figure 5), while after exposure to 800 °C, cracks appeared along the height of the concrete specimen (Figure 6). The number of cracks in the specimens of the reference SCC mixture increases with the increase in temperature. According to Yüzer et al. [29], at the moment of cooling, calcium oxide CaO passes into calcium hydroxide $Ca(OH)_2$, which then travels through the pores of the concrete leading to an increase in volume and the appearance of larger cracks.

Figure 5. Mixture SCC-R—occurrence of cracks at the bottom of the specimens (400 °C and 600 °C).

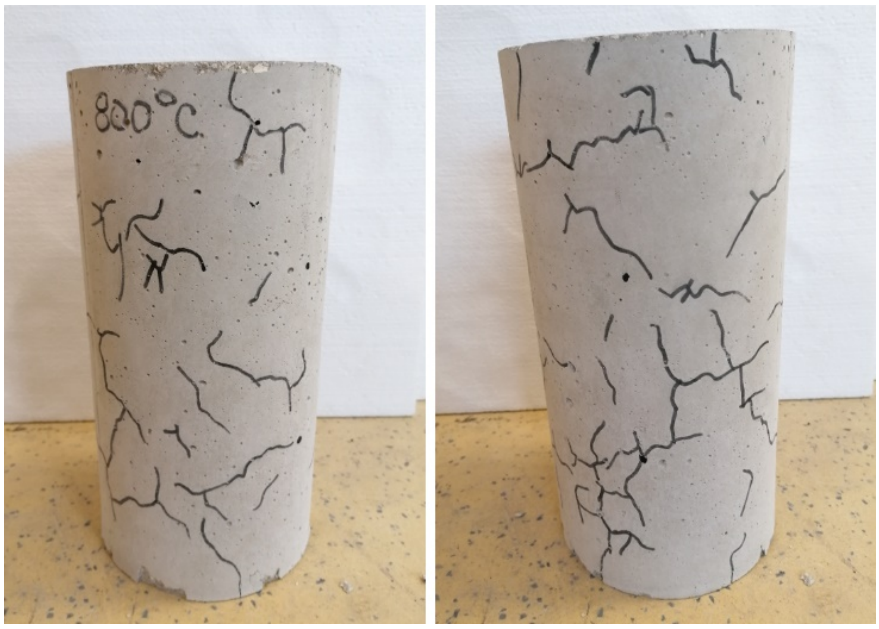

Figure 6. Mixture SCC-R—occurrence of cracks along with the entire height of the specimens (800 °C).

No cracks were observed on the surface of specimens from mixtures SCC-10-0 and SCC-15-5, which is not in agreement with previous studies where specimens with recycled rubber had visible cracks on the surface after exposure to 600 and 800 °C [30–32]. The difference in the behaviour compared to other studies can be explained as follows:

(i) a longer drying process of specimens, leading to a lower amount of water absorbed in the concrete pores before testing, consequently leading to lower internal stresses and a smaller number of cracks on the surface of concrete specimens after exposure to high temperatures;
(ii) in previous studies [31,33] the heating regime was 5 and 10 °C/min, while this study applied RILEM recommendations [65] for an increase of 0.5 °C/min, which means that in those studies a similar amount of water present (bound or unbound) needs to evaporate in less time, thus creating higher pore pressures and more cracks.

Similar to the scaling effect, the reduction in the number of cracks in SCC specimens with recycled rubber contributes to the durability of concrete by preserving the thickness of the protective layer, preventing the penetration of aggressive substances into the internal structure, and protecting the reinforcement from external influences.

The change in colour of SCC specimens was controlled by visual inspection after exposure to high temperatures (Figure 7). Table 5 provides a proposal for visual recognition of concrete conditions after exposure to high temperatures, enabling the determination to which temperature the concrete was exposed. Similar to previous test results [31,32], the specimens become pink-grey, brown-grey, or dark-grey after being exposed to 200, 400, and 600 °C, respectively. However, specimens SCC-15-5 exposed to a temperature of 400 °C become brown-grey with brown spots, which can be explained by the fact that more recycled rubber, containing carbon, has burned out [31]. When specimens were exposed to 800 °C, the colour of the concrete changed from light-grey to white-grey, regardless of whether recycled rubber is one of the concrete components or not. During exposure of specimen SCC-15-5 to a temperature higher than 400 °C smoke was observed, caused by decomposition and combustion of large quantities of recycled rubber, which mainly consists of carbon and hydrogen [30]. Smoke has not been reported in any of the previous studies. When exposing SCC specimens of mixtures SCC-R and SCC-10-0 to temperatures higher than 400 °C, the amount of smoke is negligible. In terms of user safety, 10% replacement of natural aggregate with recycled rubber would be optimal, so as not to additionally endanger human health in case of fire or high temperatures. However, it should be noted that structures without additional layers such as plaster on the inside or layers of thermal insulation on the outside are rarely constructed. Taking this into consideration, it can be assumed that in the early stages of fire the appearance of smoke would not play a crucial role in such a hazard scenario, and later stages of fire present structural danger which is far more threatening.

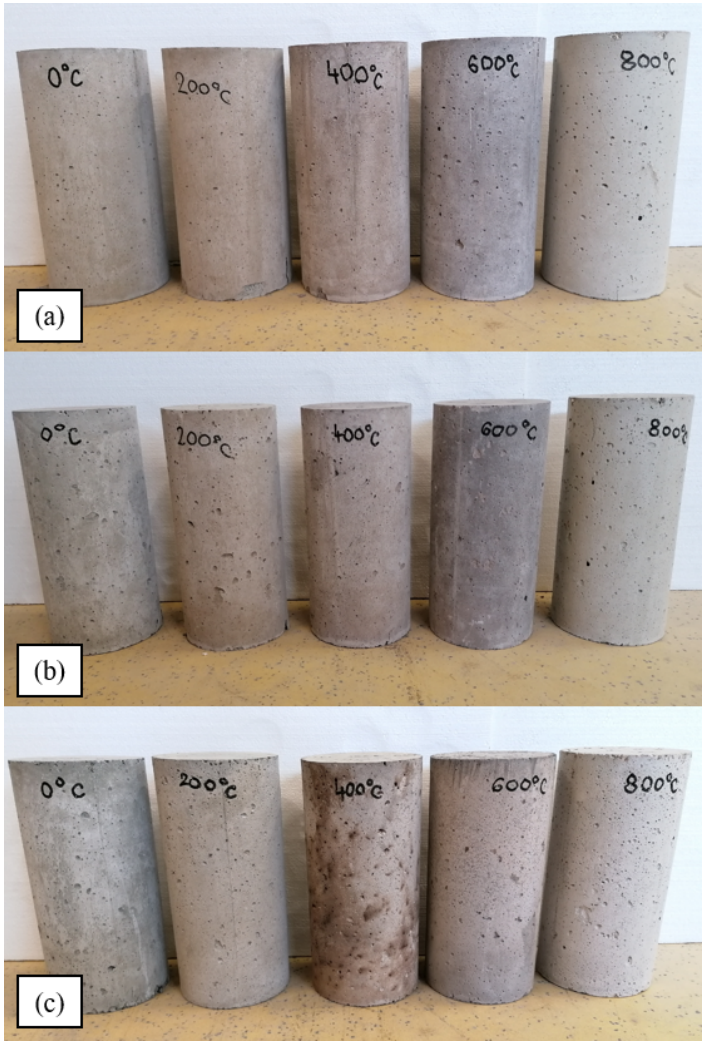

Figure 7. Colour change after specimen exposure to high temperatures: (**a**) SCC-R, (**b**) SCC-10-0, (**c**) SCC-15-5.

Table 5. Proposal for visual recognition of concrete condition after exposure to high temperatures.

Mixture	High Temperature				
	20 °C	**200 °C**	**400 °C**	**600 °C**	**800 °C**
SCC-R	light-grey	pink-grey	brown-grey	dark-grey	white-grey
SCC-10-0			brown-grey		
SCC-15-5			brown-grey with brown spots		

Figure 8 shows the average residual mass of the specimens after exposure to high temperatures. There is a slightly higher mass loss in concrete specimens with rubber, similar to the results reported by [32,33]. This is due to the combustion and decomposition of recycled rubber, consequently leading to an increase in the weight loss of the concrete specimens. Mass loss at temperatures up to 150 °C is also present due to the evaporation of the capillary water and the water contained in the C-S-H gel. At higher temperatures, chemically bound water is released from concrete during the decomposition of calcium hydrate into calcium oxide and water [33]. However, it should be noted that the differences in mass loss of SCC mixtures with recycled rubber compared to the reference SCC mixture are quite small. At 512 °C calcium hydroxide ($Ca(OH)_2$) decomposes into water (H_2O) and calcium oxide (CaO) [73], leading to the largest decrease in average residual mass for all mixtures between temperatures of 600 and 800 °C since the value of mass loss depends on the duration of the temperature load [74,75]. It can be concluded that the composition of the concrete mixture, which is partially modified with the addition of rubber and silica fume, has no significant effect on increasing or decreasing specimen mass loss when exposed to the same high temperature. Increasing the temperature to which the concrete is exposed decreases the mass, which indicates an increase in the porosity of concrete and thus a decrease in mechanical properties.

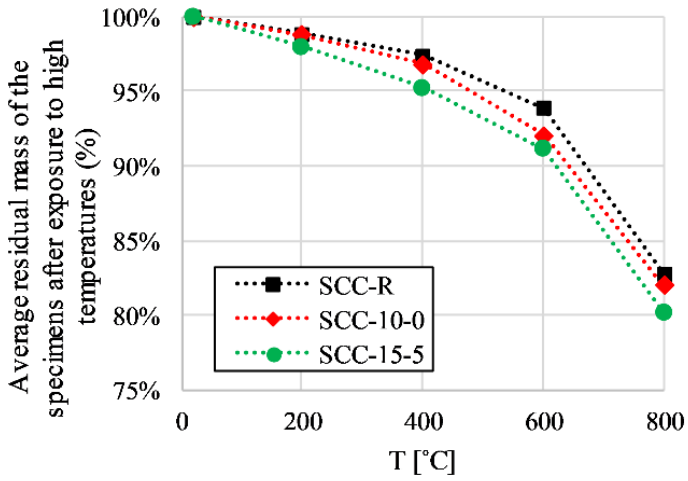

Figure 8. Average residual mass of the specimens after exposure to high temperatures.

Measuring the UPV has great potential for testing structural members exposed to high temperatures or fire, especially since it is a non-destructive testing method. Connecting the value of the UPV with the assessment of the residual mechanical properties of concrete exposed to high temperatures is an important parameter to determine the maximum temperature to which the concrete was exposed during temperature loads. UPV was measured on six SCC cylinders, with three measurements per specimen, before testing the compressive strength and modulus of elasticity to keep the specimens complete and undamaged. Average UPV values after exposure to high temperatures are presented in Table 6. A decrease in UPV value with an increase in temperature and rubber content in concrete has been observed [30,33], which indicates that high temperatures cause significant damage to the cement paste.

Table 6. Average UPV values after exposure to high temperatures and quality of SCC based on the UPV values after exposure to high temperature.

T (°C)	SCC-R		SCC-10-0		SCC-15-5	
	UPV (m/s)	Quality	UPV (m/s)	Quality	UPV (m/s)	Quality
20	4930.74	excellent	4325.28	very good	4090.53	very good
200	4441.18	very good	3979.19	very good	3754.96	very good
400	3805.65	good	3433.98	good	3070.44	good
600	3170.77	good	2815.41	generally poor	2489.31	generally poor
800	2653.37	generally poor	2476.88	generally poor	2075.88	extremely poor

A decrease in the UPV value with an increase in rubber content (and consequently a decrease in natural aggregate) can be explained by the lower specific gravity of recycled rubber compared to natural aggregate [76], which increases the time required for the ultrasonic pulse to pass through the concrete specimen. If the specimens are exposed to temperatures higher than 200 °C, the reduction in the UPV value can be explained by the increased number of discontinuities and air cavities caused by high temperatures and combustion of recycled rubber [30,33]. Additionally, the decrease in the UPV values with the increase in temperature is directly related to the decrease in the mechanical properties of the concrete. Therefore, an estimation of the high-temperature effect on the mechanical properties can be performed using the UPV values, providing insight into the structural capacity of a reinforced concrete member. To evaluate the quality of SCC after exposure to high temperatures, the obtained average UPV values were compared with the limit values given in ASTM C597 [77] (Table 6). It can be concluded that the specimens can be classified as good-quality concrete up to an exposure temperature of 400 °C, after which the concrete quality for the SCC-10-0 and SCC-15-5 mixtures becomes generally or extremely poor, while the SCC-R mixture after exposure to a temperature of 600 °C still shows good quality.

The SCC specimens exposed to high temperatures were tested on a pressure kiln with a capacity of 3000 kN. Extensometers were used to measure deformations when testing the modulus of elasticity, while LVDTs were used to obtain the stress–strain relation during compressive strength testing. For the compressive strength testing SCC specimens were first subjected to a stress of 0.05 MPa, defined in the RILEM recommendations as a preload level, and then loaded with a stress rate of 0.5 MPa/s until failure. The stress regime of the specimens on which the secant modulus of elasticity under pressure was tested was according to EN 12390-13 [60]. For further analysis, three parameters were taken from the stress–strain relation:

(i) compressive strength ($f_c = \sigma_{max}$);
(ii) strain (ε) at the maximum stress;
(iii) slope of the curve.

Test results are presented in Table 7 and Figures 9 and 10, while Figures 11–15 show a comparison of the stress–strain curves for three specimens of the investigated SCC mixtures, for all test temperatures (total of nine curves per graph).

Table 7. Test results of the mechanical properties of the SCC specimens exposed to high temperatures (MPa).

Property	Mixture	Temperature				
		20 °C	200 °C	400 °C	600 °C	800 °C
$f_c = \sigma_{max}$	SCC-R	55.55	52.60	35.89	33.57	20.25
	SCC-10-0	40.83	38.43	29.87	21.57	15.44
	SCC-15-5	33.42	33.52	21.92	15.95	8.88
E	SCC-R	41,454.86	34,352.50	29,190.56	17,003.44	10,470.33
	SCC-10-0	26,882.57	26,251.25	16,667.61	10,437.80	6048.28
	SCC-15-5	27,268.08	21,372.97	12,551.73	7673.42	4741.43

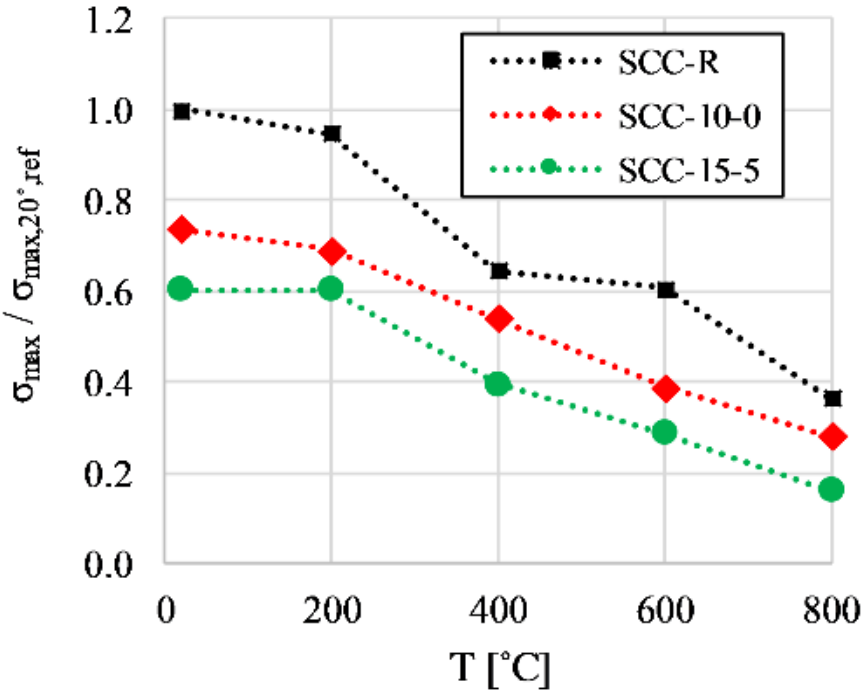

Figure 9. Normalised values of the compressive strength ($f_c = \sigma_{max}$) concerning the value of the modulus of elasticity of the reference SCC mixture at $T = 20$ °C.

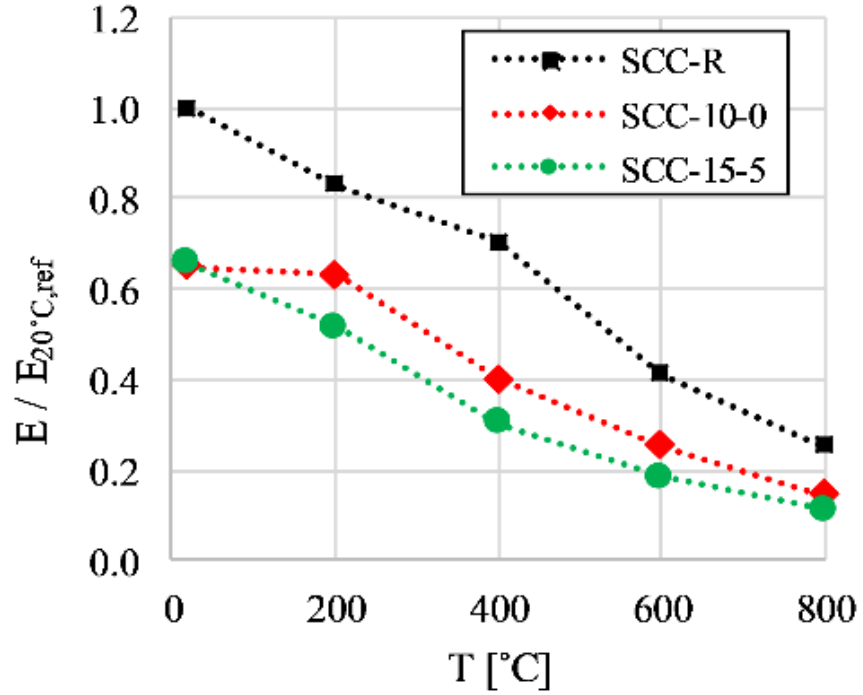

Figure 10. Normalised values of the modulus of elasticity (E) concerning the value of the modulus of elasticity of the reference SCC mixture at $T = 20$ °C.

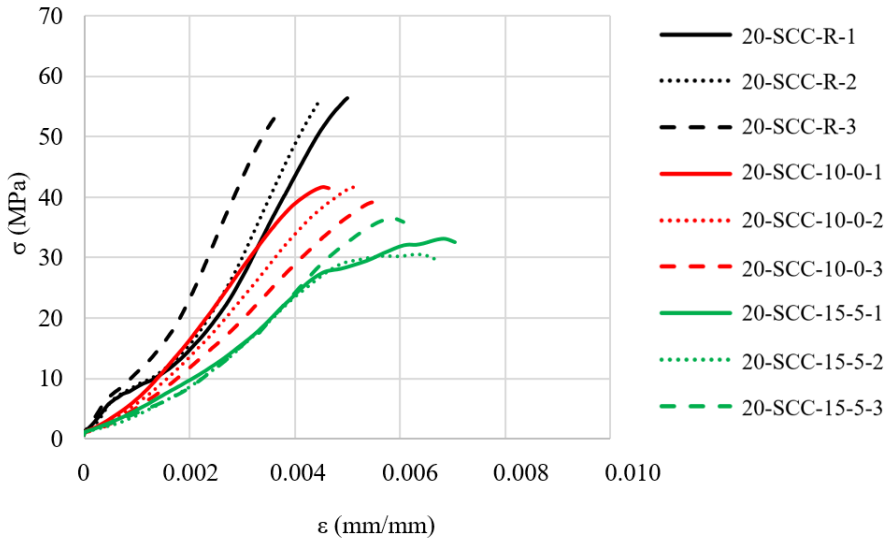

Figure 11. Compressive stress–strain relation of the SCC specimens at room temperature.

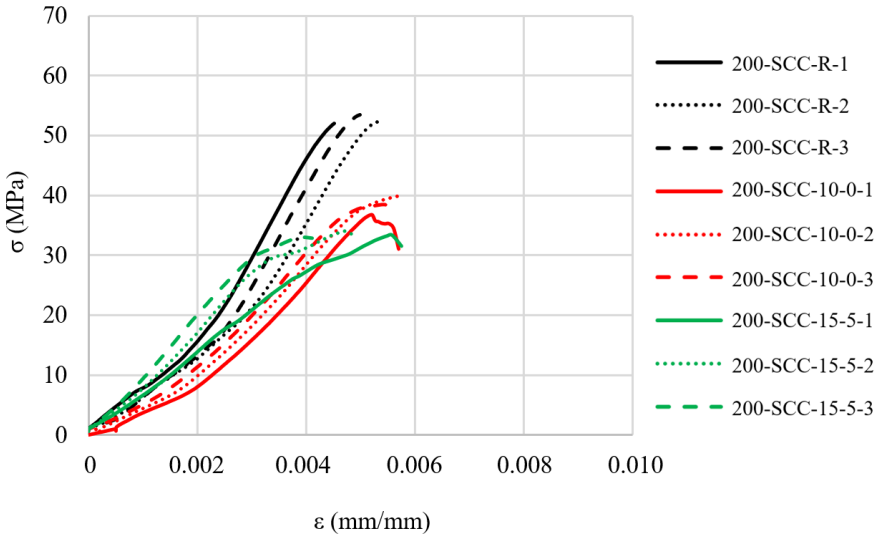

Figure 12. Compressive stress–strain relation of the SCC specimens exposed to 200 °C.

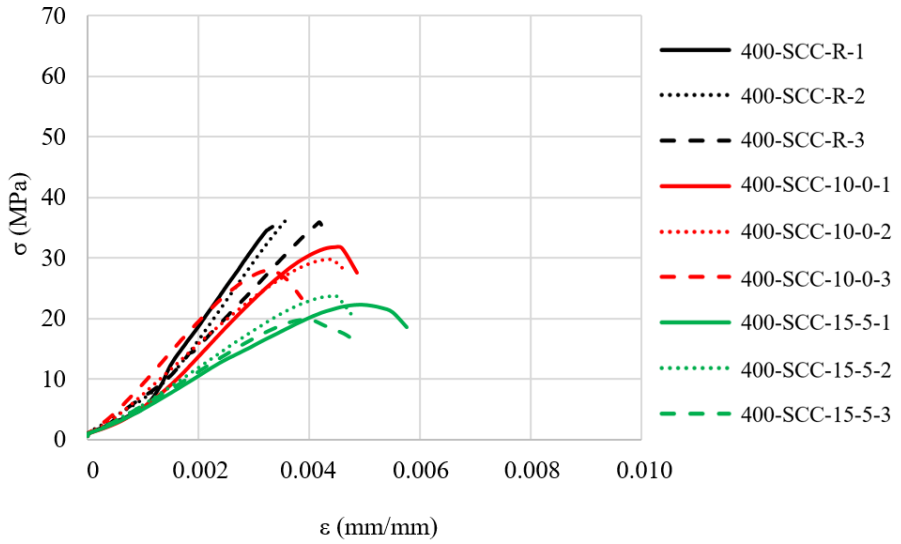

Figure 13. Compressive stress–strain relation of the SCC specimens exposed to 400 °C.

Regardless of the high temperature, the compressive strength values of the SCC specimens were highest for the reference SCC mixture, consistent with previous investigations of SCRC [37], traditional rubberised concrete [31,33,78], and mortar with recycled rubber [30]. The primary reason is the lower compressive strength of recycled rubber compared to natural aggregate [78]. The analysis of the test results shows that the decrease in the compressive strength of SCC-R was most pronounced after exposure to 400 °C. Compared to the compressive strength values at 20 °C, the reduction in compressive strength was 35%, while the same reduction was 27% for concrete specimens with 10% rubber. The average compressive strength values for all three mixtures tested after exposure to 600 and 800 °C were higher than 15 and 8 MPa, respectively. Unlike previous tests where concrete specimens exposed to 750 °C could not be tested due to their poor condition [33], all specimens maintained their integrity after exposure to 800 °C. A positive effect of silica fume on the compressive strength of concrete specimens with 15% rubber was observed after exposure to a temperature of 200 °C where the relative decrease in compressive strength was negligible. However, at temperatures above 400 °C specimens with 10% rubber maintained strength better than specimens with 15% rubber. Therefore, it can be concluded that at temperatures above 400 °C the positive effect of silica fume could not compensate for the negative impact of a 15% replacement level of fine aggregate with recycled rubber. At high temperatures, the free water in the capillary pores of the concrete and the water in the C-S-H gel evaporates [30], and at temperatures higher than 400 °C, C-S-H gels decompose [33,37], explaining why the highest reduction in compressive strength is at 400 °C. At similar temperatures, rubber burns, which increases the porosity of the concrete specimens [30], resulting in a weaker structure and a reduction in the ability to transmit compressive forces in specimens during testing. A smaller relative decrease in compressive strength of the SCC-10-0 specimens may be due to an easier release of water vapour from concrete specimens with rubber. Considering the resistance of concrete to high temperatures and the values of residual compressive strengths of concrete specimens, it can be suggested that the maximum replacement level of recycled rubber in SCC should be 10% of the total volume of fine aggregate to maintain the stability and structural capacity of reinforced concrete members in case of their exposure to high temperatures.

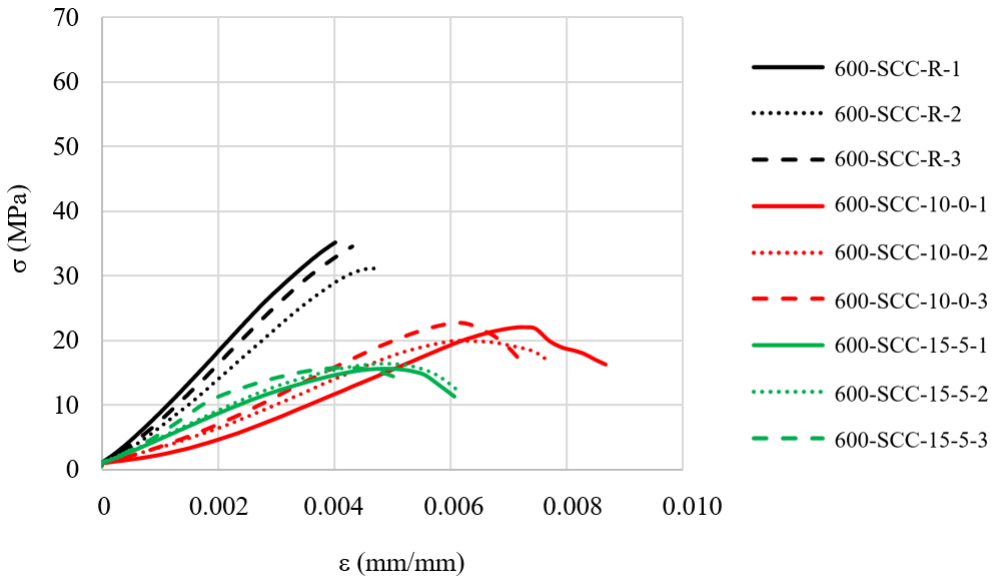

Figure 14. Compressive stress–strain relation of SCC specimens exposed to 600 °C.

The values of the modulus of elasticity of the specimens of all concrete mixtures were above 20 GPa even after exposure to a temperature of 200 °C. For specimens of the SCC mixtures SCC-10-0 and SCC-15-5, the modulus of elasticity value falls below 20 GPa only after the specimens were exposed to temperatures higher than 400 °C. Compared

to SCC specimens with 10 and 15% recycled rubber, the modulus of elasticity of the reference SCC mixture was higher at all exposure temperatures. However, observing the relative reduction in the modulus of elasticity at high temperatures to those at room temperature (E/E_{20} °C), it can be concluded that the specimens of the reference SCC mixture experienced the highest reduction in the modulus of elasticity after exposure to a high temperature of 200 °C, while at the same temperature specimens with 10% rubber had a relative reduction of only 2%. For specimens with 10% rubber exposed to temperatures of 400 °C, this ratio of relative reduction was more pronounced. The specimens SCC-15-5 had the most pronounced relative reduction in the modulus of elasticity at all high temperatures. These trends coincide with the strong correlation of compressive strength and modulus value in general when it comes to concrete, but only a small number of researchers have studied the change in the static modulus of elasticity of concrete with rubber with similar observations [33]. Therefore, it can be concluded that the same causal effects of the high temperature determined for compressive strength are valid for the elastic modulus.

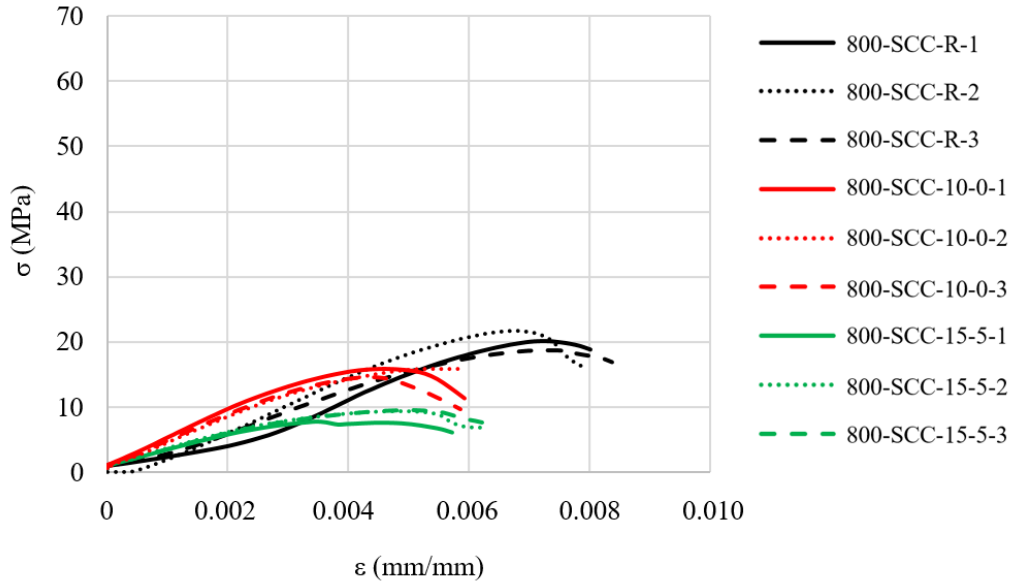

Figure 15. Compressive stress–strain relation of the SCC specimens exposed to 800 °C.

The relationships between the average values of UPV and mechanical properties at different exposure temperatures are shown in Figures 16 and 17, and they clearly show that there is good agreement between the linear regression analysis equation and the experimental results. This leads to the possibility of estimating the compressive strength and modulus of elasticity based on the UPV values.

To date, no research has been conducted on the stress–strain relation of ordinary or SCC with recycled rubber after exposure to high temperatures. From the stress–strain relations shown in Figures 11–15, it can be concluded that the slopes of the curves, and thus the values of the modulus of elasticity and deformation at maximum force, are in the function of three parameters:

(i) the temperature to which the specimens were exposed;
(ii) percentage of recycled rubber;
(iii) percentage of silica fume.

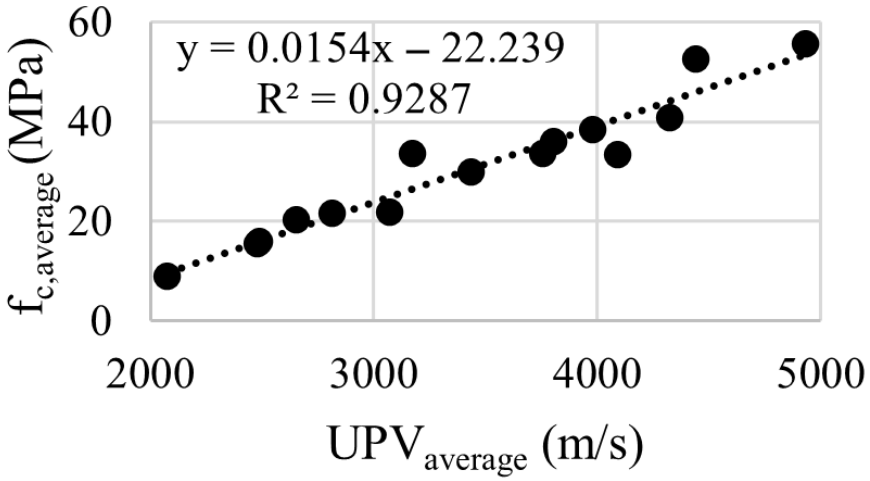

Figure 16. UPV-f_c relation for specimens of the investigated SCC mixtures.

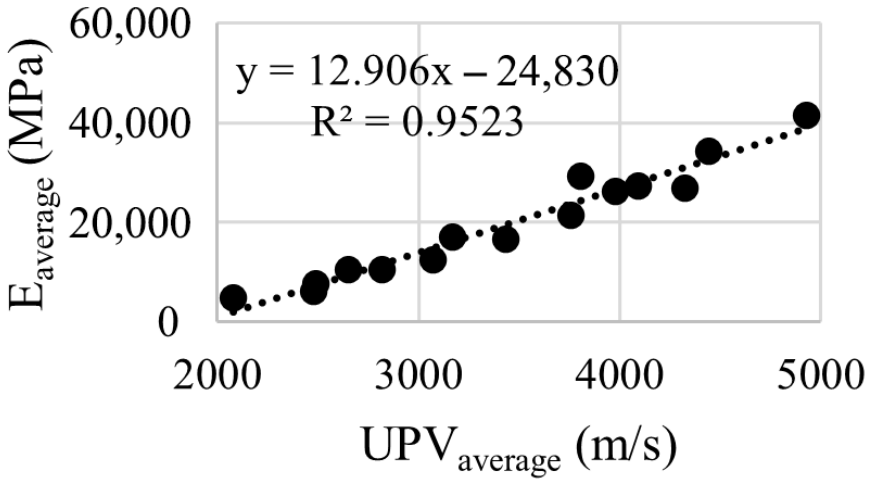

Figure 17. UPV-*E* relation for specimens of the investigated SCC mixtures.

The trend that the higher the percentage level of recycled rubber, the lower the slope of the curve (lower modulus of elasticity) applies to specimens exposed to temperatures up to 600 °C. For the specimens exposed to a temperature of 800 °C the slope of the curve is unaffected by the amount of recycled rubber. When comparing the deformations at maximum force at the same temperatures, increasing rubber content increases the deformation at maximum force; however, an exception to this is at a temperature load of 800 °C where specimens of the reference SCC mixture have the maximum average deformation at maximum force. This can be attributed to the fact that with rubber total combustion there is no aid in deformability. Aside from the highest temperature, concrete specimens without recycled rubber show less deformability than concrete specimens with recycled rubber. Increased deformability of concrete specimens with recycled rubber can contribute to the improvement of the resistance of reinforced concrete members to seismic activities in the form of more ductile fracture scenarios through the creation of a large number of smaller cracks, thus increasing the dissipation ability of reinforced concrete members.

Figure 18 shows typical modes of specimen failure exposed to high temperatures, under a compressive strength test. Explosive failure and spalling were characteristics of specimens from the reference concrete mixture, while a ductile fracture with a large number of minor cracks was observed in specimens of the concrete mixtures SCC-10-0 and SCC-15-5. This behaviour, also observed in other studies [72,79], can be explained by the positive impact of recycled rubber, which provides additional elasticity to the concrete and increases its resistance to tensile stresses. However, it should be noted that the level of

explosive spalling in specimens of the reference mixture SCC-R decreases with the increase in exposed temperature, especially when specimens were exposed to 800 °C. This behaviour can be explained by the weaker internal structure of the SCC caused by water loss and decomposition of the C-S-H gel. The appearance of reduced explosive spalling can be characterised as a positive contribution of recycled rubber to the development of concrete structural members. Figure 19 shows the results of the residual compressive strength test obtained experimentally when testing concrete at high temperatures, compared with the compressive strength values as a function of the concrete temperature according to the model for calcareous and siliceous aggregates that are given in EN 1992-1-2 [80].

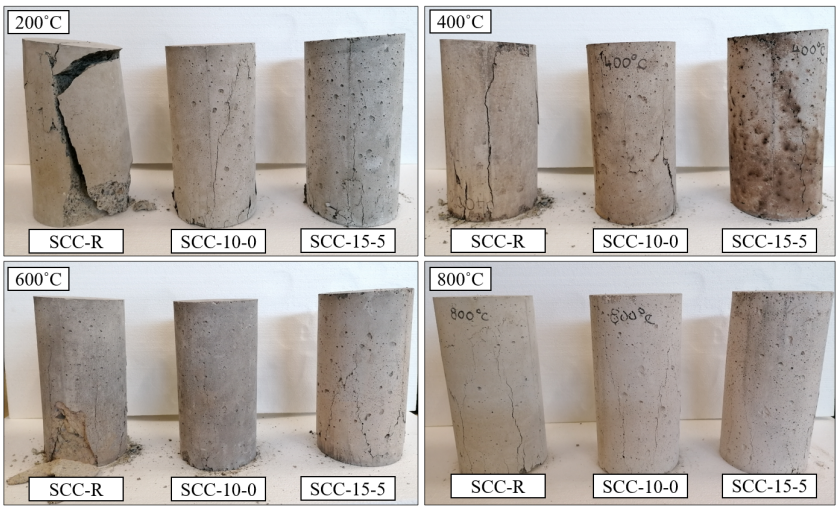

Figure 18. Failure modes of the SCC specimens exposed to high temperatures.

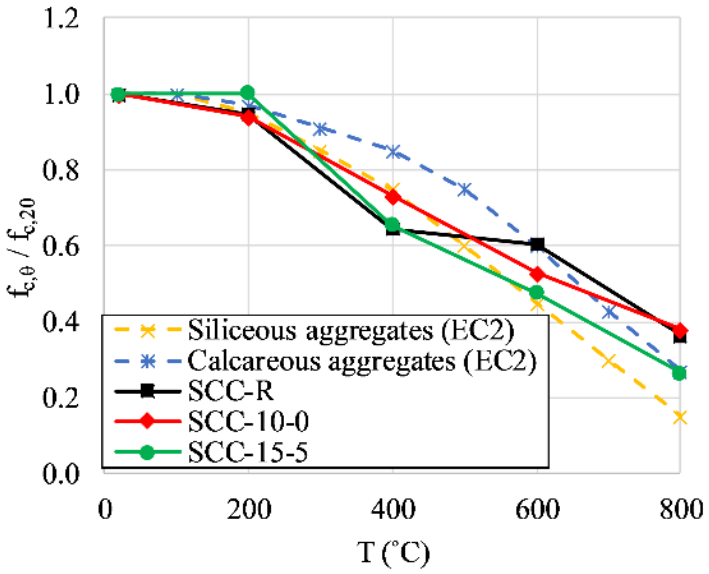

Figure 19. Ratios of residual compressive strength and compressive strength at room temperature ($f_{c,\theta} / f_{c,20}$), as a function of concrete temperature, given in EN 1992-1-2.

According to Figure 19, several conclusions can be drawn:

(i) The test results of the three concrete mixtures show similarities to those of the models for calcareous and siliceous aggregates. The maximum percentage difference between the calcareous aggregate model and the ratio values obtained experimentally is around 20% (SCC-R and SCC-15-5 at 400 °C), while the maximum percentage difference between the siliceous aggregate model and the ratio values obtained experimentally is 22.8% (SCC-10-0 at 800 °C);

(ii) It can be concluded that the models given by EN 1992-1-2 can be used for these concrete mixtures, but are not mostly unsafe;
(iii) It is proposed to further investigate the mixtures of SCC-R and SCC-15-5 at 400 °C since a sharp drop in the $f_{c,\theta}/f_{c,20}$ ratios was observed. The sudden drop in compressive strength of the mixture with 15% rubber content can be explained by the combustion process and the accelerated decomposition of rubber after reaching its melting point, while the sharp drop in compressive strength of SCC-R concrete at 400 °C can be explained by the decomposition of the C-S-H gel.

3.3.6. Thermal Conductivity

Test results of thermal conductivity for three investigated SCC mixtures are presented in Table 8. Individual and mean values of thermal conductivity are the lowest for specimens SCC-15-5 and the highest for specimens SCC-R. The mean values of thermal conductivity for the specimens SCC-10-0 and SCC-15-5 are 20% and 39% lower, respectively, than the mean value of thermal conductivity for the specimens of the reference concrete mix. Similar results can be found in the existing literature where thermal conductivity was tested on specimens of mortar with rubber [34,35], SCC with rubber [36], and ordinary concrete with rubber [28]. The decrease in the value of thermal conductivity of concrete by increasing the amount of recycled rubber in the concrete can be explained by better thermal insulation properties of recycled rubber, i.e., a lower value of thermal conductivity of rubber (0.16–0.50 W/mK) [28,35,36] compared to natural aggregate (1.5–5.20 W/mK) [28,35]. However, the total thermal conductivity of concrete also depends on the volume and distribution of pores and trapped air at the interface of the aggregate and cement paste [35], which is increased by replacing the natural aggregate with rubber. This is due to the fact that air (0.025 W/mK) has a lower thermal conductivity value than concrete [36]. If it is assumed that SCRC would be used for the production of reinforced concrete members of a heated building, increasing the rubber content above 15% would further increase the positive effect on reducing the thermal conductivity of the materials and reducing the amount of aggregate used from natural resources. This could positively affect two basic construction requirements, namely, rational energy management and heat conservation in buildings and the sustainable use of natural resources. However, to use SCRC in reinforced concrete structural members, it is necessary to define the maximum percentage of recycled rubber that would contribute to the improvement of heat consumption and sustainable use of natural resources, while maintaining adequate mechanical resistance and stability. Since the compressive strength of mixtures SCC-10-0 and SCC-15-5 are similar, i.e., 30 MPa, the maximum content of the recycled rubber in reinforced concrete structural elements of up to 15% is proposed.

Table 8. Test results of thermal conductivity for the investigated SCC mixtures.

Mixture	Specimen	λ_i (W/mK)	$\lambda_{average}$ (W/mK)	St. Dev. (W/mK)	CoV (%)
SCC-R	1	1.67	1.64	0.021	1.30
	2	1.65			
	3	1.62			
	4	1.64			
SCC-10-0	1	1.31	1.31	0.003	0.24
	2	1.31			
	3	1.30			
	4	1.31			
SCC-15-5	1	1.06	1.01	0.064	6.35
	2	0.91			
	3	1.02			
	4	1.04			

3.4. Microstructural Analysis

The microstructural analysis of 15 concrete specimens and one recycled rubber specimen was performed using the JEOL SEM JSM-IT200 scanning electron microscope. Microstructural analysis of the concrete specimens was made to determine the *recycled rubber–cement paste* interface on specimens exposed to high temperatures. Recycled rubber was investigated to determine its morphology. Figures 20–34 show micrographs of the observed 15 concrete specimens. Concrete specimens with recycled rubber showed a weaker bond at the *recycled rubber–cement paste* interface than the bond at the interface *natural aggregate–cement paste interface*. Microscopic analysis shows cracks in the interface of *recycled rubber–cement paste*, consequently increasing the porosity of the concrete [35], increasing the gas and water permeability and reducing the compressive strength. Inhomogeneous surfaces and sharp edges of crumb rubber lead to a decrease in the workability of concrete and an increase in the air content in concrete [76], which in SCC reflects the need for an increased content of superplasticizers. The effect of high temperatures on recycled rubber was very noticeable in specimens SCC-10-0-400-deg and SCC-10-0-600-deg (specimens exposed to temperatures of 400 and 600 °C), where recycled rubber cracked or disintegrated, and the empty space in the *recycled rubber–cement paste* interface was further increased. Furthermore, the width of the cavities between the recycled rubber and the cement paste increased with increasing temperature. The described behaviour can be associated with a smaller relative decrease in the compressive strength of concrete specimens with recycled rubber compared to concrete specimens of the reference mixture exposed to high temperatures. Partial combustion and reduction in the volume of recycled rubber led to an increased number of additional channels through which water vapour could pass, consequently causing less pore pressure on the internal structure of the concrete specimens, thus providing less destruction and scaling of the concrete.

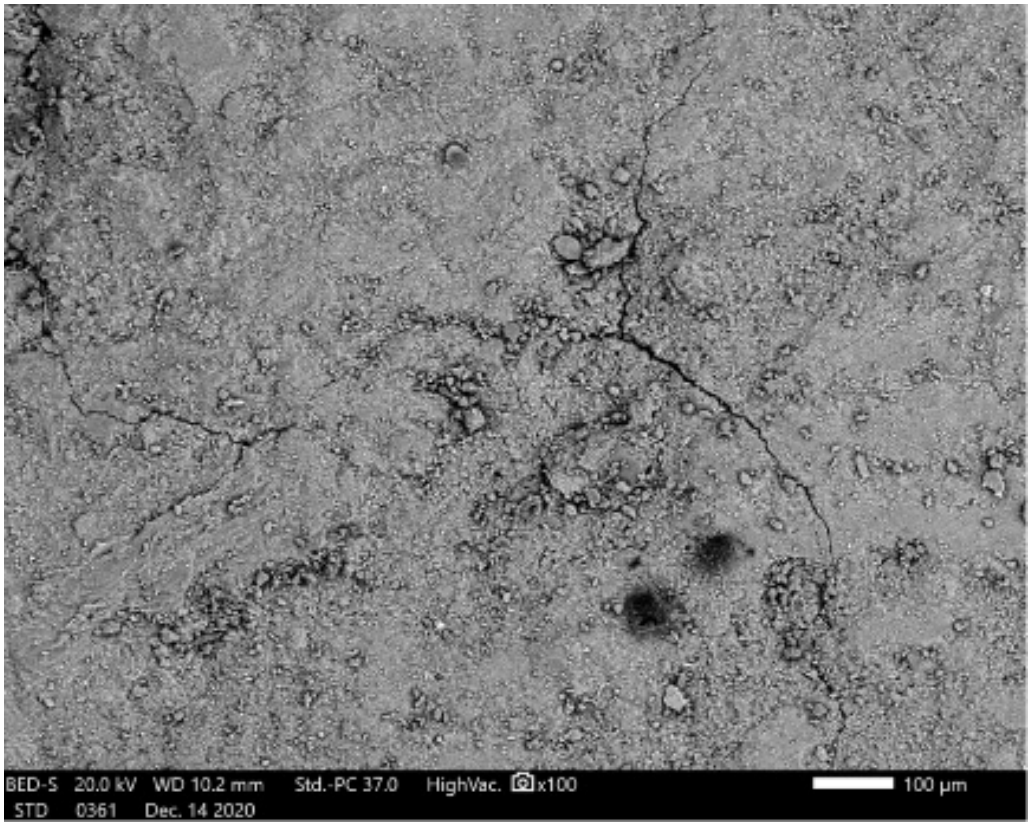

Figure 20. Micrograph SCC-R-20-deg; magnification of 100×.

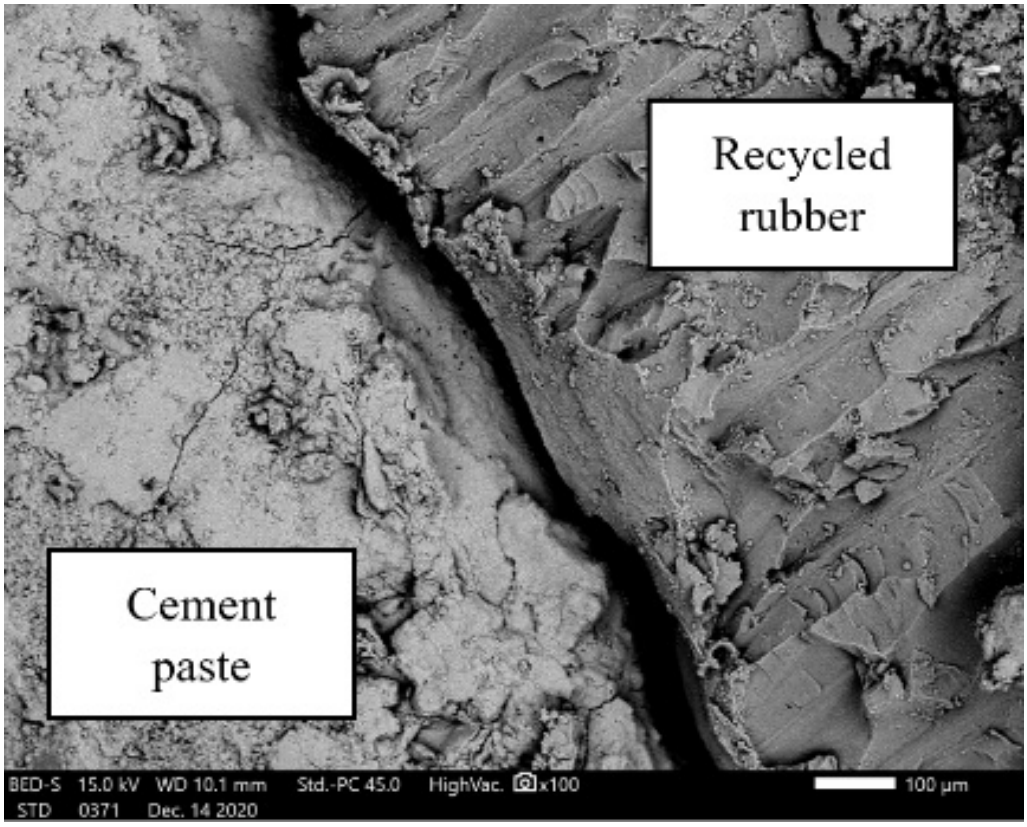

Figure 21. Micrograph SCC-10-0-20-deg; magnification of 100×.

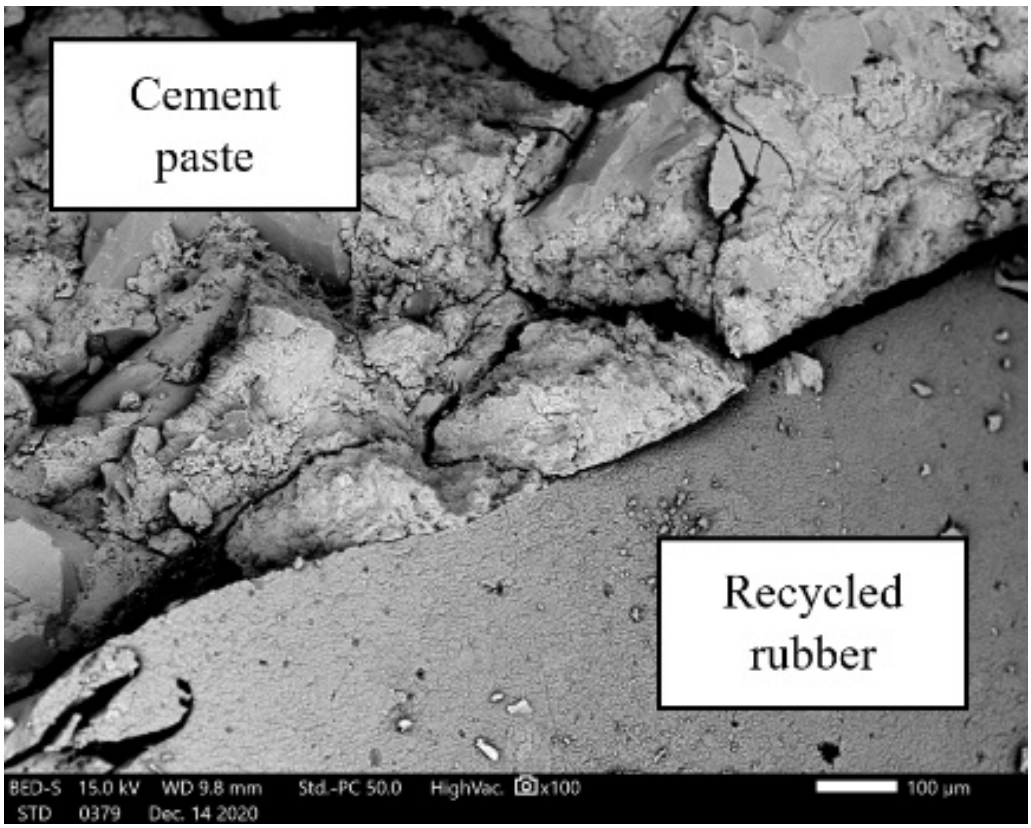

Figure 22. Micrograph SCC-15-5-20-deg; magnification of 100×.

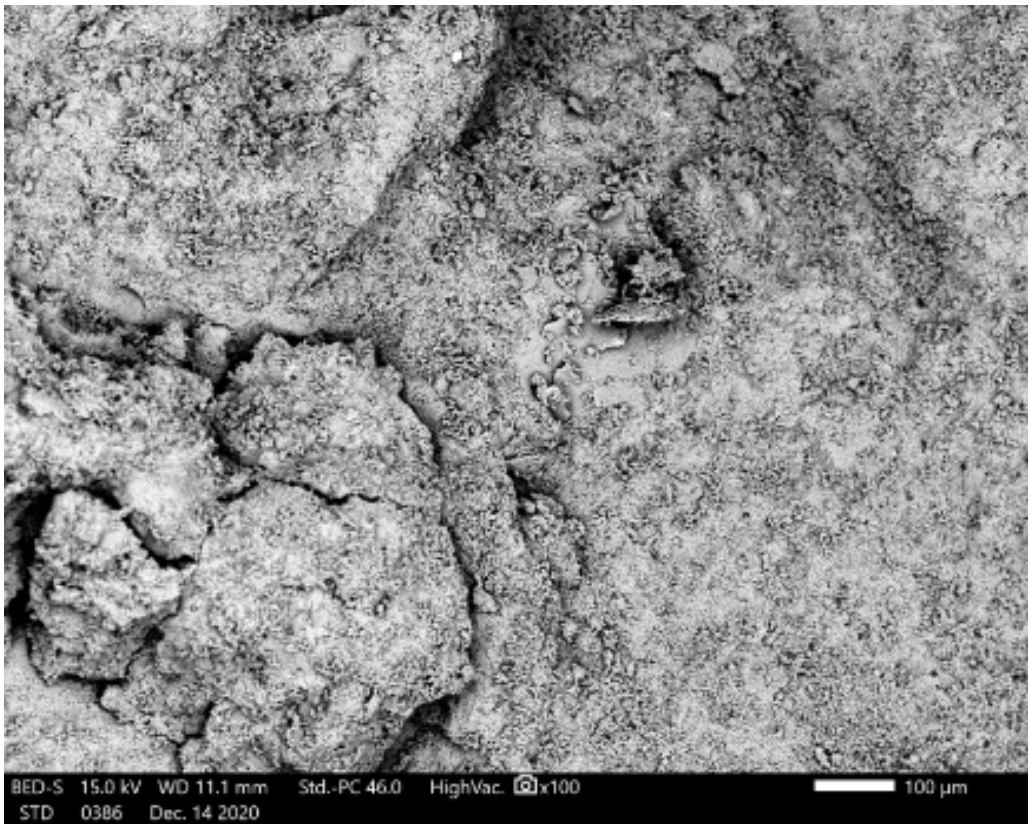

Figure 23. Micrograph SCC-R-200-deg; magnification of 100×.

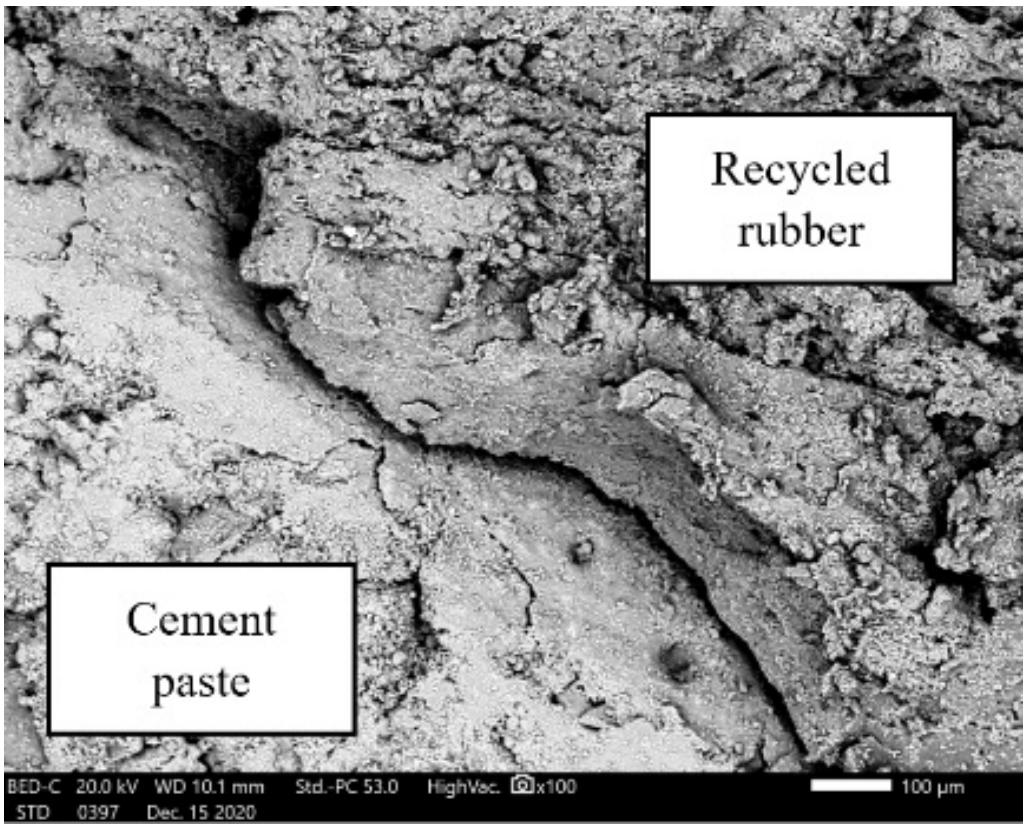

Figure 24. Micrograph SCC-10-0-200-deg; magnification of 100×.

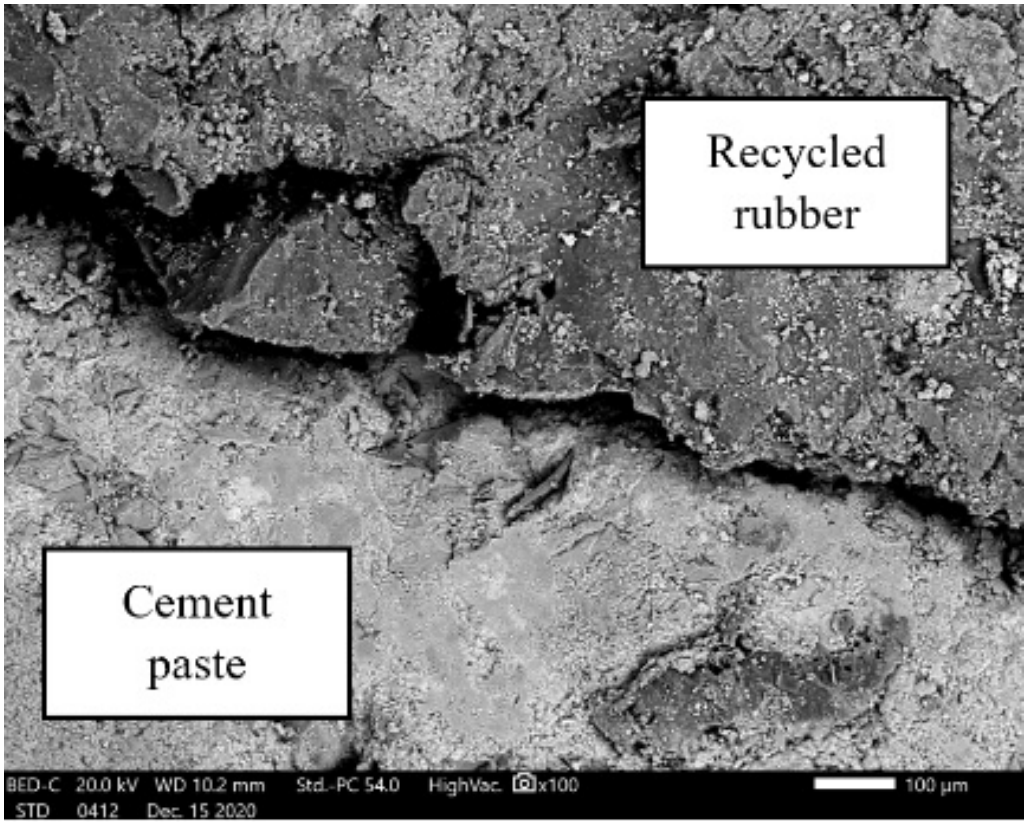

Figure 25. Micrograph SCC-15-5-200-deg; magnification of 100×.

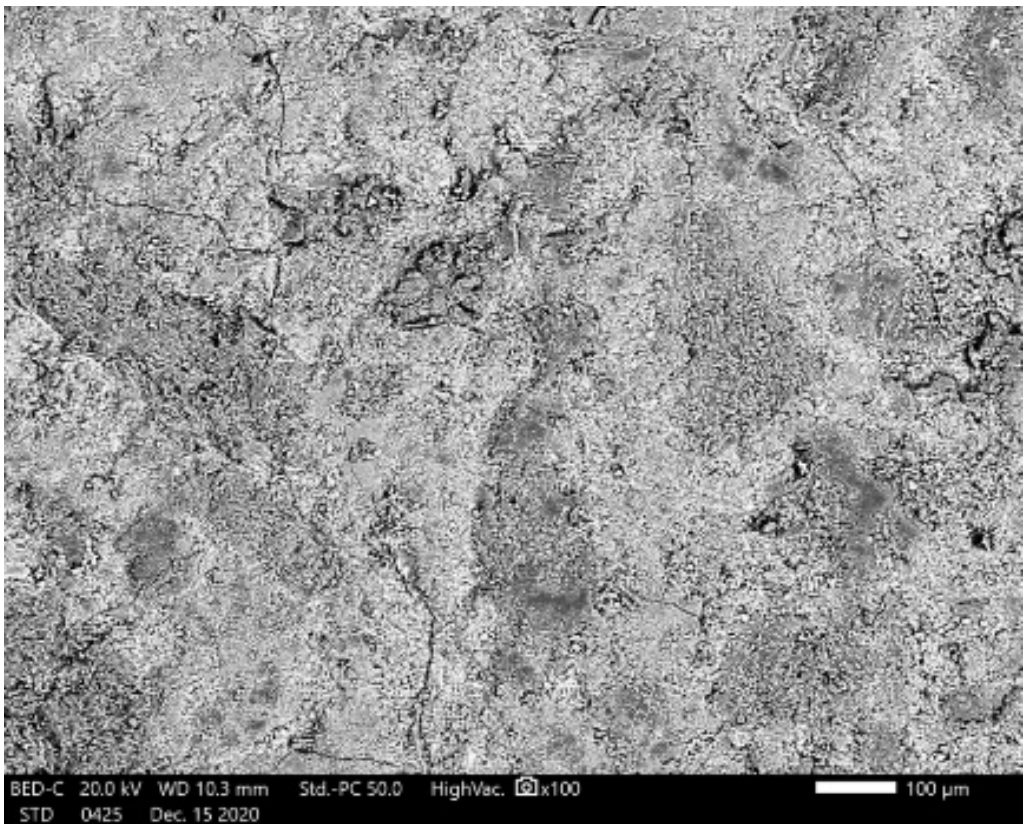

Figure 26. Micrograph SCC-R-400-deg; magnification of 100×.

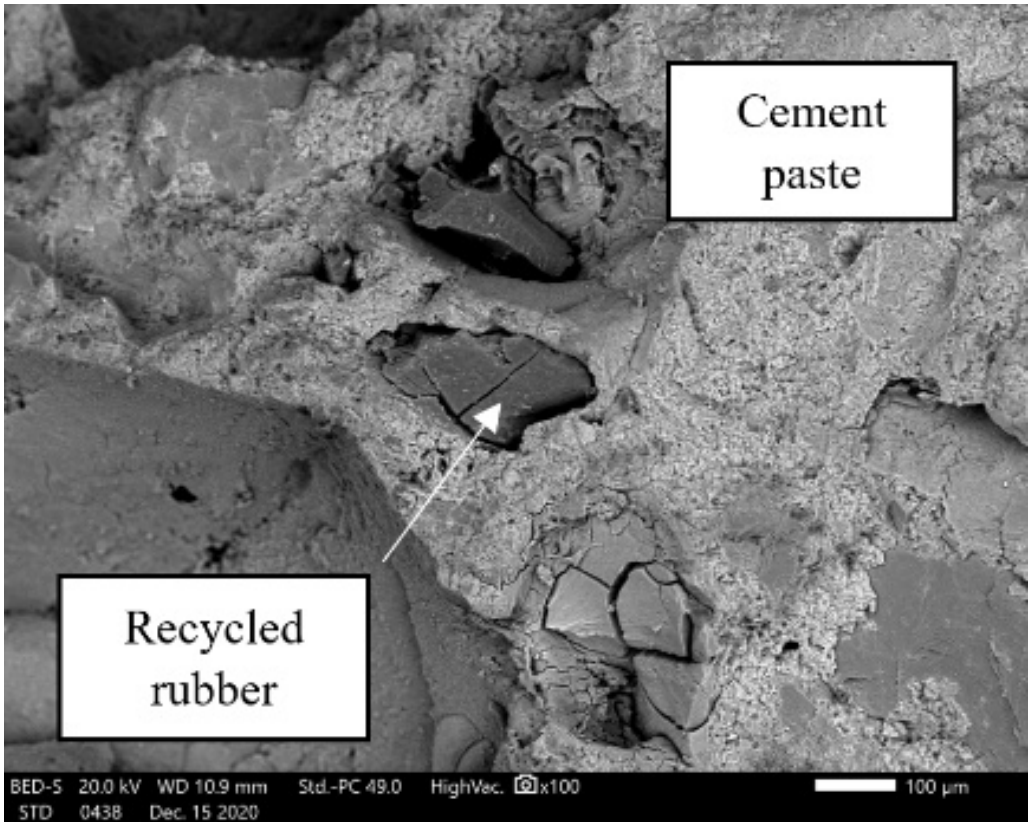

Figure 27. Micrograph SCC-10-0-400-deg; magnification of 100×.

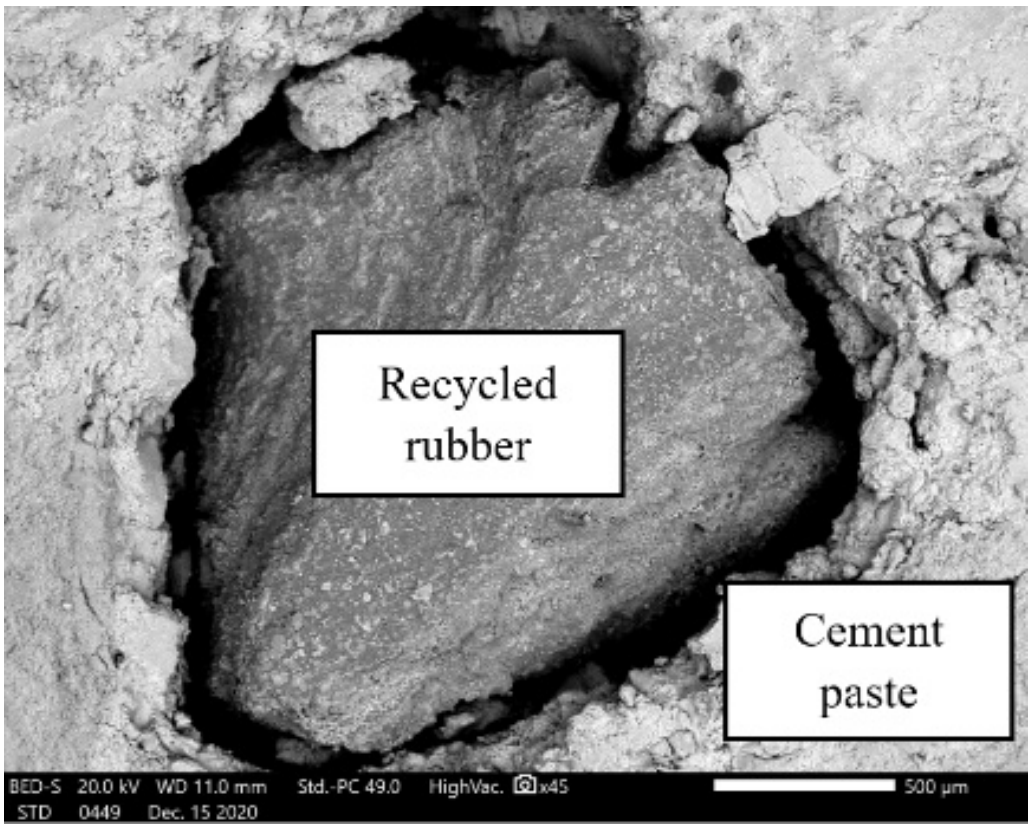

Figure 28. Micrograph SCC-15-5-400-deg; magnification of 45×.

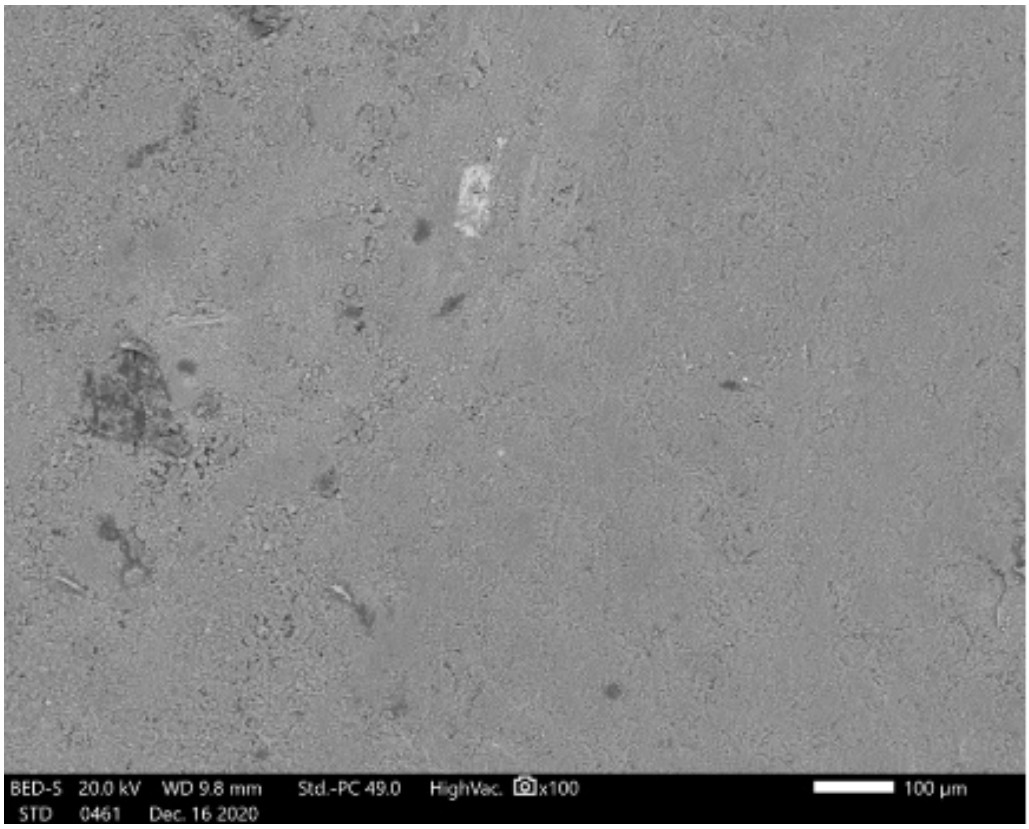

Figure 29. Micrograph SCC-R-600-deg; magnification of 100×.

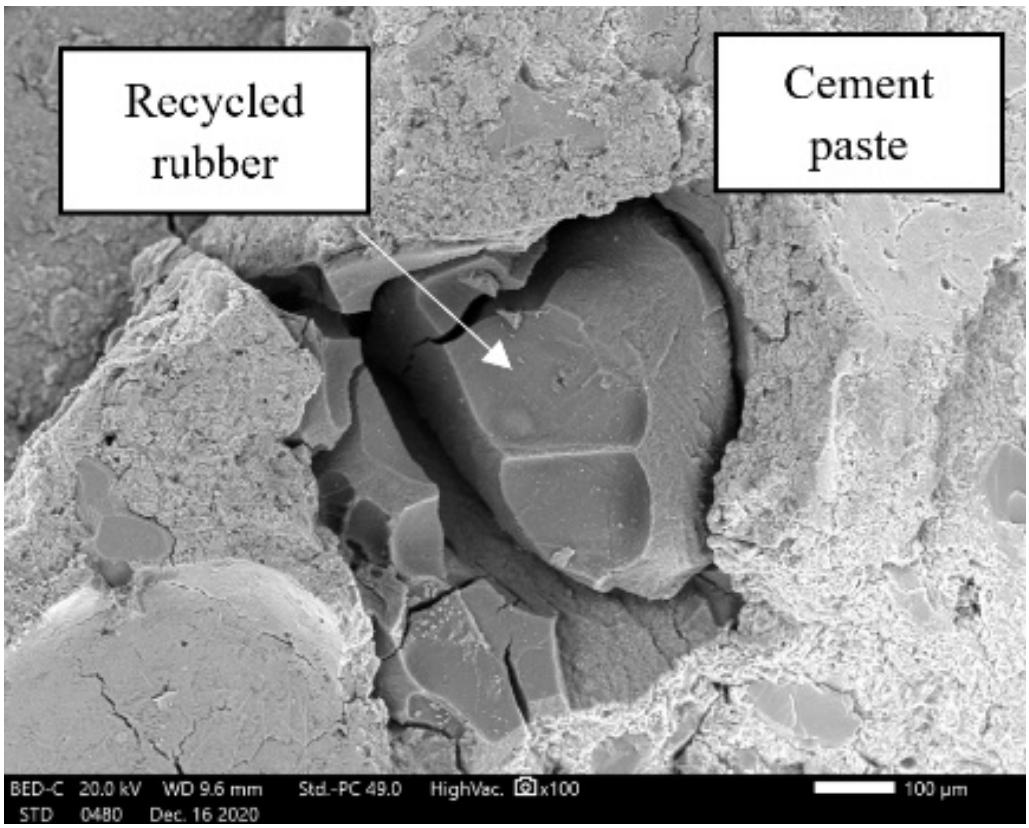

Figure 30. Micrograph SCC-10-0-600-deg; magnification of 100×.

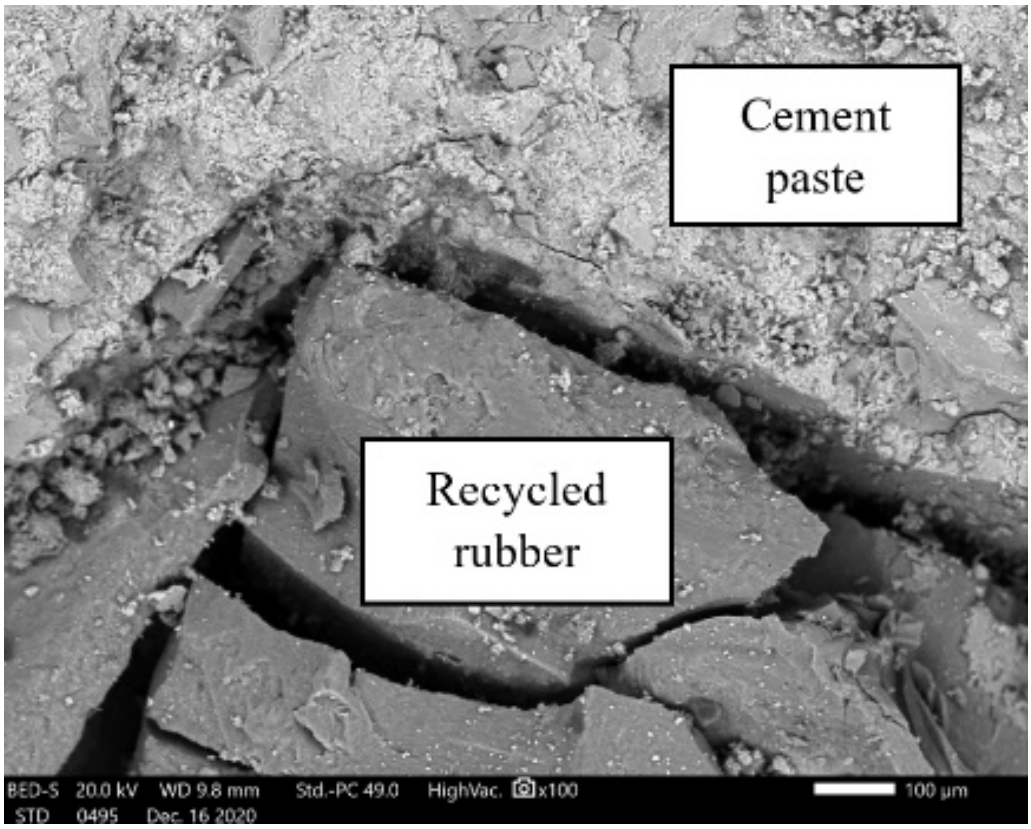

Figure 31. Micrograph SCC-15-5-600-deg; magnification of 100×.

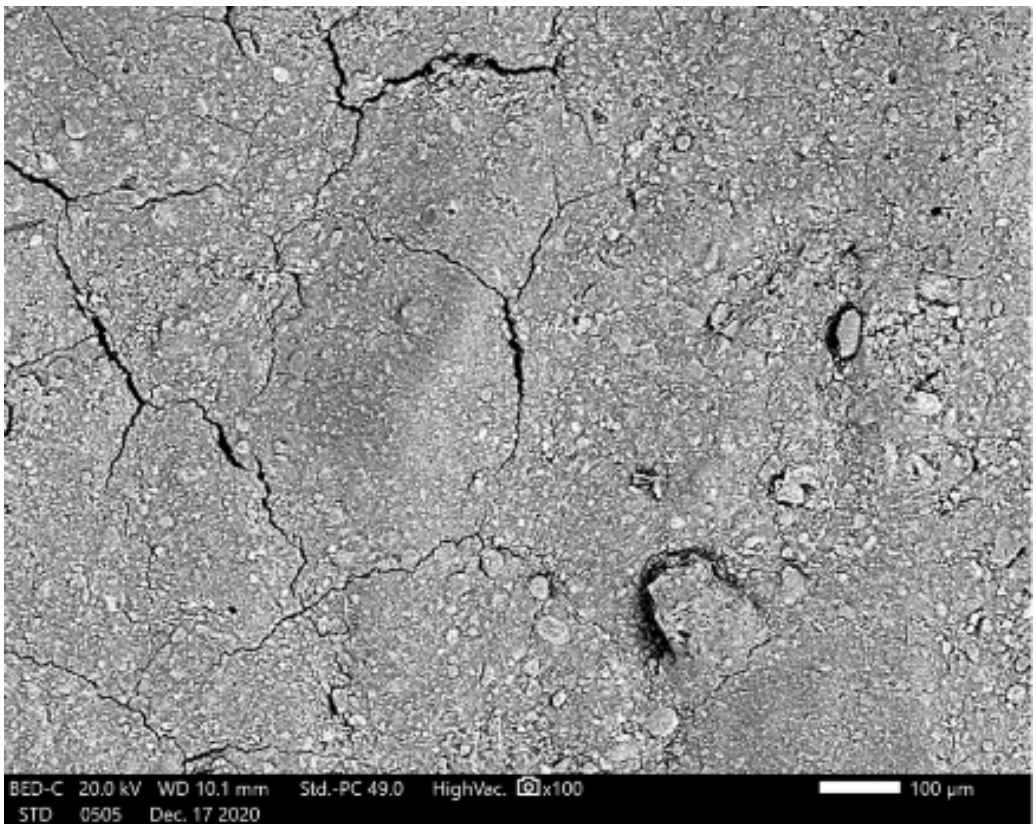

Figure 32. Micrograph SCC-R-800-deg; magnification of 100×.

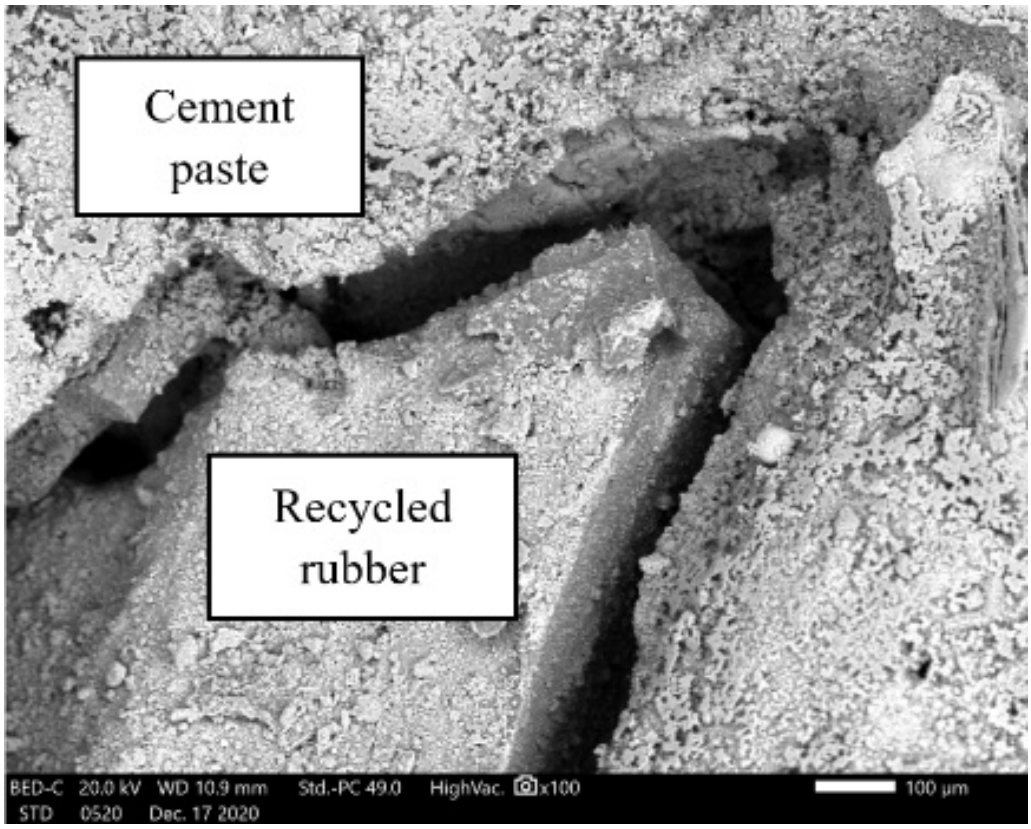

Figure 33. Micrograph SCC-10-0-800-deg; magnification of 100×.

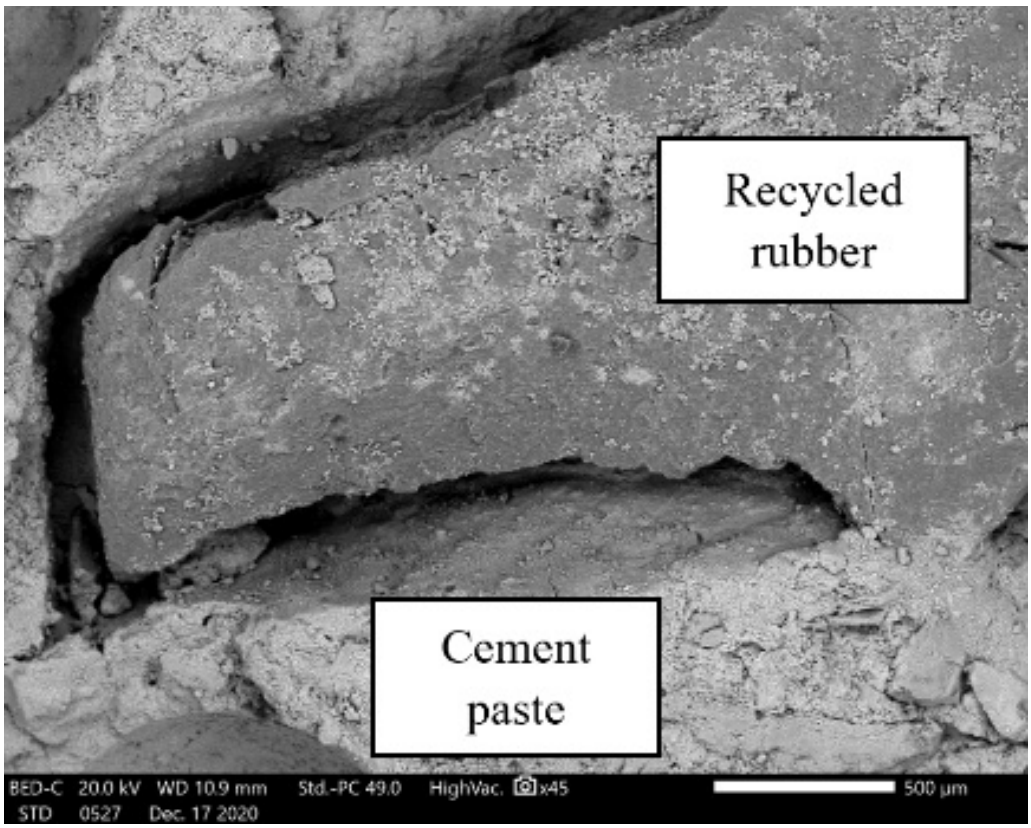

Figure 34. Micrograph SCC-15-5-800-deg; magnification of 45×.

During the microstructural analysis, microcracks were observed in concrete specimens without recycled rubber (Figure 35). Microcracks were not observed in the investigated concrete specimens containing recycled rubber, which can be explained by a higher porosity rate and lower internal stresses caused by the pore pressure of water vapour, compared to concrete specimens without rubber. Regardless of the applied high temperature, the use of recycled rubber, which burns at high temperatures and reduces its volume, provides additional free space to accept water vapour pressures caused by the evaporation of water, eliminating the appearance of microcracks. This phenomenon is also associated with a smaller relative drop in the compressive strength of the rubberised concrete compared to the conventional concrete. This additionally confirms previous results and implications. Figure 36 shows a micrograph of the recycled rubber showing sharp edges and irregular rubber shapes, the main reason for the reduced workability of the fresh concrete and the need for an additional amount of superplasticizer to achieve the desired class of slump flow. The irregular shape of the recycled rubber is the main cause of the increased concrete porosity. However, the advantage of using fine crumb rubber was highlighted by Chylík et al. [24], where it was shown that the finer fraction contributes to the formation of air pores of optimal size and spacing in the hardened concrete,the main reason why the concrete mix containing a finer fraction of recycled rubber had better resistance to the freeze–thaw cycles.

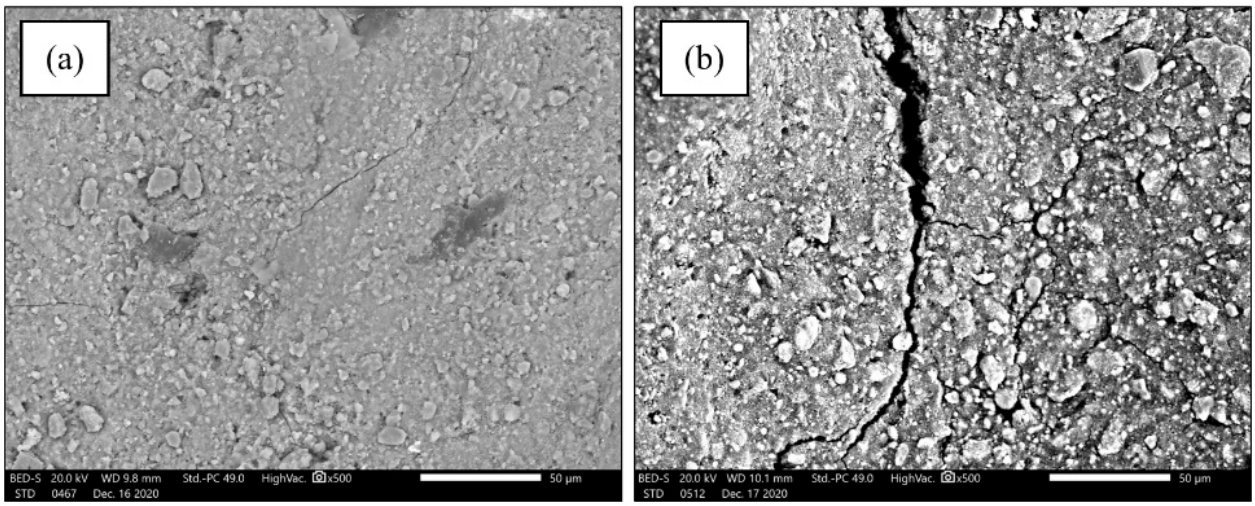

Figure 35. Occurrence of microcracks: (**a**) SCC-R-600-deg; (**b**) SCC-R-800-deg; magnification of 500×.

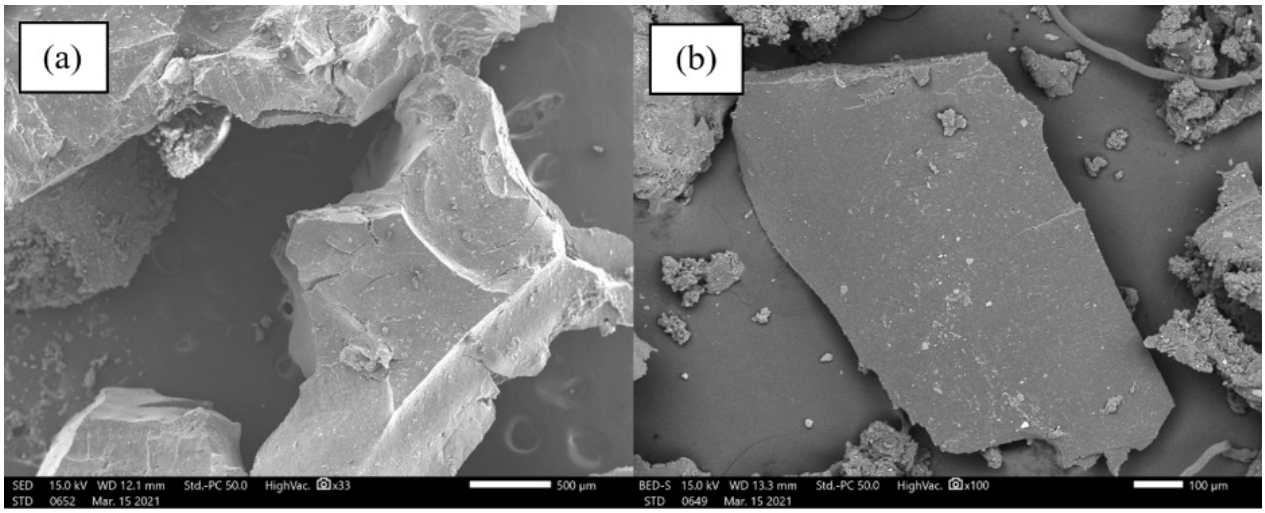

Figure 36. SEM images of different fractions of recycled rubber; magnification of (**a**) 33× and (**b**) 100×.

4. Conclusions

This study investigated the properties of selected optimal mixtures of self-compacting concrete (SCC) with recycled rubber. The research included an investigation of the durability properties, thermal properties, and microstructural analysis of SCC with recycled rubber. Several conclusions can be drawn from the experimental results:

- Based on the value of the gas permeability coefficient, all concrete mixtures can be classified as medium-quality concrete.
- It is recommended to limit the use of SCC with recycled rubber to design situations where the material is not exposed to direct contact with pressurized water, i.e., in structurally reinforced concrete members located above the level of the finished terrain.
- Recycled rubber contributes to the potential reduction in the number and size of cracks in hardened concrete, which in turn can lead to the greater durability of the concrete and lower the maintenance costs during the design life of the building.
- Freeze–thaw resistance is increased by using recycled rubber in SCC which can lead to savings as less aerant is needed.
- Recycled rubber preserves the surface structure of concrete after and during exposure to high temperatures, thus improving the durability of the concrete and reinforcement in the form of reduced cracks, preserving the protective layer.
- It is possible to assess the quality of the concrete using the UPV value, to estimate the effect of high-temperature exposure on concrete with and without rubber on the reduction in compressive strength and modulus of elasticity.
- Concrete with recycled rubber is a positive contributor to the development of reinforced concrete structural members with recycled rubber as it provides increased deformability, resulting in more cracks with reduced width and depth.
- The microstructural analysis confirms different explanations for the positive and negative effects of rubber in concrete exposed to high temperatures. This is confirmed by the results of the compressive strength test and modulus of elasticity test, as well as the freeze–thaw resistance test.
- Rubberized concrete has thermal properties similar to lightweight concrete, but can potentially achieve higher strengths compared to lightweight concrete, as the reduction in the strength of concrete is partly due to the reduction in its density.

After a detailed analysis of all test results of optimal mixtures at the material level, a general conclusion can be drawn that the use of recycled rubber as a substitute for natural fine aggregate in SCC is justified. In the next step, it is proposed to approach the experimental investigation of optimal mixtures of SCC with recycled rubber at the level of reinforced concrete structural members to obtain a complete picture of the impact of recycled rubber on the properties of SCC and to develop guidelines for the use of SCRC in structurally reinforced concrete members. Furthermore, it would be worthwhile to investigate the impact of SCC with recycled rubber and silica fume on carbonation and corrosion resistance, as these are important factors to consider in the design of durable and long-lasting concrete structures.

Author Contributions: Conceptualisation, R.B.; Methodology, R.B. and I.M.; Investigation, R.B., I.M. and T.D.; Writing—original draft, R.B.; Writing— review & editing, I.M., T.D. and M.G.; Visualization, R.B.; Supervision, I.M., T.D. and M.G.; Project administration, I.M.; Funding acquisition, I.M. All authors have read and agreed to the published version of the manuscript.

Funding: This paper was supported by the Croatian Science Foundation (HrZZ) under the project UIP-2017-05-7113 "Development of Reinforced Concrete Elements and Systems with Waste Tire Powder—ReCoTiP" [recotip.gfos.hr] (accessed on 1 May 2023), and their support is gratefully acknowledged.

Acknowledgments: The authors acknowledge the constructive comments and suggestions provided by the anonymous reviewers, which improved the manuscript's quality.

Conflicts of Interest: The authors declare no conflict of interest.

Abbreviations

The following abbreviations are used in this manuscript (in alphabetical order):

ASTM	American Society for Testing and Materials
CoV	Coefficient of Variation
CR	Crumb Rubber
C-S-H	Calcium-Silicate Hydrate
GGBFS	Ground Granulated Blast-Furnace Slag
LVDT	Linear Variable Differential Transformer
MK	Metakaolin
RILEM	Réunion Internationale des Laboratoires et Experts des Matériaux
SCC	Self-Compacting Concrete
SCM	Supplementary Cementitious Material
SCRC	Self-Compacting Rubberized Concrete
SEM	Scanning Electron Microscope
SF1, SF2, SF3	Slump Flow Classes
SLF	Silica Fume
SP	Superplasticizer
UPV	Ultrasonic Pulse Velocity
VDP1, VDP2, VDP3	Water Permeability Classes of Concrete
VMA	Viscosity-Modifying Admixture
XF2, XF4	Concrete Exposure Classes

References

1. Wellmer, F.W.; Becker-Platen, J. Sustainable development and the exploitation of mineral and energy resources: A review. *Int. J. Earth Sci.* **2002**, *91*, 723–745. [CrossRef]
2. Bleischwitz, R.; Bahn-Walkowiak, B. Aggregates and Construction Markets in Europe: Towards a Sectoral Action Plan on Sustainable Resource Management. *Miner. Energy Raw Mater. Rep.* **2007**, *22*, 159–176. [CrossRef]
3. Mohammed, S.I.; Najim, K.B. Mechanical strength, flexural behavior and fracture energy of Recycled Concrete Aggregate self-compacting concrete. *Structures* **2020**, *23*, 34–43. [CrossRef]
4. Bideci, A.; Öztürk, H.; Bideci, Ö.S.; Emiroğlu, M. Fracture energy and mechanical characteristics of self-compacting concretes including waste bladder tyre. *Constr. Build. Mater.* **2017**, *149*, 669–678. [CrossRef]
5. Uygunoğlu, T.; Topçu, İ.B. The role of scrap rubber particles on the drying shrinkage and mechanical properties of self-consolidating mortars. *Constr. Build. Mater.* **2010**, *24*, 1141–1150. [CrossRef]
6. Zaouai, S.; Makani, A.; Tafraoui, A.; Benmerioul, F. Optimization and mechanical characterization of self-compacting concrete incorporating rubber aggregates. *Asian J. Civ. Eng. (BHRC)* **2016**, *17*, 817–829.
7. Roychand, R.; Gravina, R.J.; Zhuge, Y.; Ma, X.; Youssf, O.; Mills, J.E. A comprehensive review on the mechanical properties of waste tire rubber concrete. *Constr. Build. Mater.* **2020**, *237*, 117651. [CrossRef]
8. AbdelAleem, B.H.; Hassan, A.A.A. Development of self-consolidating rubberized concrete incorporating silica fume. *Constr. Build. Mater.* **2018**, *161*, 389–397. [CrossRef]
9. Hilal, N.N. Hardened properties of self-compacting concrete with different crumb rubber size and content. *Int. J. Sustain. Built Environ.* **2017**, *6*, 191–206. [CrossRef]
10. Turatsinze, A.; Garros, M. On the modulus of elasticity and strain capacity of Self-Compacting Concrete incorporating rubber aggregates. *Resour. Conserv. Recycl.* **2008**, *52*, 1209–1215. [CrossRef]
11. Ismail, M.K.; Hassan, A.A.A. Use of metakaolin on enhancing the mechanical properties of self-consolidating concrete containing high percentages of crumb rubber. *J. Clean. Prod.* **2016**, *125*, 282–295. [CrossRef]
12. Si, R.; Wang, J.; Guo, S.; Dai, Q.; Han, S. Evaluation of laboratory performance of self-consolidating concrete with recycled tire rubber. *J. Clean. Prod.* **2018**, *180*, 823–831. [CrossRef]
13. Ismail, M.K.; Hassan, A.A.A. Impact Resistance and Mechanical Properties of Self-Consolidating Rubberized Concrete Reinforced with Steel Fibers. *J. Mater. Civ. Eng.* **2017**, *29*, 4016193. [CrossRef]
14. Najim, K.B.; Hall, M.R. Mechanical and dynamic properties of self-compacting crumb rubber modified concrete. *Constr. Build. Mater.* **2012**, *27*, 521–530. [CrossRef]
15. Khalil, E.; Abd-Elmohsen, M.; Anwar, A.M. Impact Resistance of Rubberized Self-Compacting Concrete. *Water Sci.* **2015**, *29*, 45–53. [CrossRef]
16. Miller, N.M.; Tehrani, F.M. Mechanical properties of rubberized lightweight aggregate concrete. *Constr. Build. Mater.* **2017**, *147*, 264–271. [CrossRef]
17. Thiyagarajan, S.V.; Thenmozhi, R.; Doddurani, M. Experimental behaviour of waste tyre rubber aggregate concrete under impact loading. *Iran. J. Sci. Technol. Trans. Civ. Eng.* **2014**, *38*, 251–259.

18. Youssf, O.; ElGawady, M.A.; Mills, J.E.; Ma, X. An experimental investigation of crumb rubber concrete confined by fibre reinforced polymer tubes. *Constr. Build. Mater.* **2014**, *53*, 522–532. . [CrossRef]
19. Zheng, L.; Huo, X.S.; Yuan, Y. Strength, Modulus of Elasticity, and Brittleness Index of Rubberized Concrete. *J. Mater. Civ. Eng.* **2008**, *20*, 692–699. [CrossRef]
20. Alsaif, A.; Bernal, S.A.; Guadagnini, M.; Pilakoutas, K. Durability of steel fibre reinforced rubberised concrete exposed to chlorides. *Constr. Build. Mater.* **2018**, *188*, 130–142. [CrossRef]
21. Guneyisi, E.; Gesoglu, M.; Mermerdas, K.; Ipek, S. Experimental investigation on durability performance of rubberized concrete. *Adv. Concr. Constr.* **2014**, *2*, 193–207. [CrossRef]
22. Bjegović, D.; Baričević, A.; Serdar, M. Durability properties of concrete with recycled waste tyres. In Proceedings of the 12th International Conference on Durability of Building Materials and Components Porto, Porto, Portugal, 12 April 2011; pp. 1659–1667.
23. Gupta, T.; Chaudhary, S.; Sharma, R.K. Mechanical and durability properties of waste rubber fiber concrete with and without silica fume. *J. Clean. Prod.* **2016**, *112*, 702–711. . [CrossRef]
24. Chylík, R.; Trtík, T.; Fládr, J.; Bílý, P. Mechanical properties and durability of crumb rubber concrete. *IOP Conf. Ser. Mater. Sci. Eng.* **2017**, *236*, 12093. [CrossRef]
25. Gesoğlu, M.; Güneyisi, E.; Khoshnaw, G.; İpek, S. Abrasion and freezing–thawing resistance of pervious concretes containing waste rubbers. *Constr. Build. Mater.* **2014**, *73*, 19–24. . [CrossRef]
26. Liu, H.; Wang, X.; Jiao, Y.; Sha, T. Experimental Investigation of the Mechanical and Durability Properties of Crumb Rubber Concrete. *Materials* **2016**, *9*, 172. . [CrossRef]
27. Zhu, X.; Miao, C.; Liu, J.; Hong, J. Influence of Crumb Rubber on Frost Resistance of Concrete and Effect Mechanism. *Procedia Eng.* **2012**, *27*, 206–213. [CrossRef]
28. Paine, K.A.; Dhir, R.K. Research on new applications for granulated rubber in concrete. In *Proceedings of the Institution of Civil Engineers—Construction Materials*; ICE Publishing: London, UK, 2010; Volume 163, pp. 7–17. [CrossRef]
29. Yüzer, N.; Aköz, F.; Öztürk, L.D. Compressive strength–color change relation in mortars at high temperature. *Cem. Concr. Res.* **2004**, *34*, 1803–1807. . [CrossRef]
30. Guelmine, L.; Hadjab, H.; Benazzouk, A. Effect of elevated temperatures on physical and mechanical properties of recycled rubber mortar. *Constr. Build. Mater.* **2016**, *126*, 77–85. [CrossRef]
31. Marques, A.M.; Correia, J.R.; de Brito, J. Post-fire residual mechanical properties of concrete made with recycled rubber aggregate. *Fire Saf. J.* **2013**, *58*, 49–57. [CrossRef]
32. Mousa, M.I. Effect of elevated temperature on the properties of silica fume and recycled rubber-filled high strength concretes (RHSC). *HBRC J.* **2017**, *13*, 1–7. [CrossRef]
33. Gupta, T.; Siddique, S.; Sharma, R.K.; Chaudhary, S. Effect of elevated temperature and cooling regimes on mechanical and durability properties of concrete containing waste rubber fiber. *Constr. Build. Mater.* **2017**, *137*, 35–45. . [CrossRef]
34. Fadiel, A.; Rifaie, F.A.; Abu-Lebdeh, T.; Fini, E. Use of crumb rubber to improve thermal efficiency of cement-based materials. *Am. J. Eng. Appl. Sci.* **2014**, *7*, 1–11. [CrossRef]
35. Eiras, J.N.; Segovia, F.; Borrachero, M.V.; Monzó, J.; Bonilla, M.; Payá, J. Physical and mechanical properties of foamed Portland cement composite containing crumb rubber from worn tires. *Mater. Des.* **2014**, *59*, 550–557. . [CrossRef]
36. Jedidia, M.; Gargouria, A.; Daoud, A. Effect of Rubber Aggregates on the Thermophysical Properties of Self-Consolidating Concrete. *Int. J. Therm. Environ. Eng.* **2014**, *8*, 1–7. [CrossRef]
37. Topçu, I.B.; Bilir, T. Experimental investigation of some fresh and hardened properties of rubberized self-compacting concrete. *Mater. Des.* **2009**, *30*, 3056–3065. [CrossRef]
38. Bušić, R.; Štirmer, N.; Miličević, I. Effect of tire powder and wood biomass ash on properties of self-compacting concrete. In Proceedings of the International Conference on Sustainable Materials, Systems and Structures (SMSS 2019), Rovinj, Croatia, 20–22 March 2019; RILEM Publications SARL: Bagneux, France, 2019; pp. 539–546.
39. Bušić, R.; Benšić, M.; Miličević, I.; Strukar, K. Prediction Models for the Mechanical Properties of Self-Compacting Concrete with Recycled Rubber and Silica Fume. *Materials* **2020**, *13*, 1821. [CrossRef]
40. Miličević, I.; Hadzima Nyarko, M.; Bušić, R.; Simonović Radosavljević, J.; Prokopijević, M.; Vojisavljević, K. Effect of Rubber Treatment on Compressive Strength and Modulus of Elasticity of Self-Compacting Rubberized Concrete. ICACM 2021: International Conference on Advanced Construction Materials, IRC 2021 X. International research conference proceedings. *World Acad. Sci. Eng. Technol. J. Struct. Constr. Eng.* **2021**, *15*, 131–134.
41. Bušić, R.; Miličević, I. *Influence of Waste Tire Rubber on Fresh and Hardened Properties of Self-Compacting Rubberized Concrete (SCRC)*; Springer International Publishing: Berlin/Heidelberg, Germany, 2020; pp. 3–10.
42. Ismail, M.K.; Hassan, A.A.A. Ductility and Cracking Behavior of Reinforced Self-Consolidating Rubberized Concrete Beams. *J. Mater. Civ. Eng.* **2017**, *29*, 04016174. [CrossRef]
43. Wang, L.; Jin, M.; Guo, F.; Wang, Y.; Tang, S. Pore Structural and Fractal Analysis of the Influence of Fly Ash and Silica Fume on the Mechanical Property and Abrasion Resistance of Concrete. *Fractals* **2021**, *29*, 2140003. [CrossRef]
44. Afroughsabet, V.; Ozbakkaloglu, T. Mechanical and durability properties of high-strength concrete containing steel and polypropylene fibers. *Constr. Build. Mater.* **2015**, *94*, 73–82. [CrossRef]

45. Nasr, D.; Behforouz, B.; Borujeni, P.R.; Borujeni, S.A.; Zehtab, B. Effect of nano-silica on mechanical properties and durability of self-compacting mortar containing natural zeolite: Experimental investigations and artificial neural network modeling. *Constr. Build. Mater.* **2019**, *229*, 116888. [CrossRef]
46. Meng, W.; Khayat, K.H. Mechanical properties of ultra-high-performance concrete enhanced with graphite nanoplatelets and carbon nanofibers. *Compos. Part Eng.* **2016**, *107*, 113–122. [CrossRef]
47. Salehi, H.; Mazloom, M. Opposite effects of ground granulated blast-furnace slag and silica fume on the fracture behavior of self-compacting lightweight concrete. *Constr. Build. Mater.* **2019**, *222*, 622–632. [CrossRef]
48. Ahmad, S.; Umar, A.; Masood, A.; Nayeem, M. Performance of self-compacting concrete at room and after elevated temperature incorporating Silica fume. *Adv. Concr. Constr.* **2019**, *7*, 31–37. [CrossRef]
49. Benaicha, M.; Belcaid, A.; Alaoui, A.H.; Jalbaud, O.; Burtschell, Y. Effects of limestone filler and silica fume on rheology and strength of self-compacting concrete. *Struct. Concr.* **2019**, *20*, 1702–1709. [CrossRef]
50. Štirmer, N.; Banjad Pečur, I. Projektiranje sastava samozbijajućeg betona. *Građevinar* **2009**, *61*, 321–329.
51. Skazlić, M.; Vujica, M. Environmentally-friendly self-compacting concrete. *Gradjevinar* **2012**, *64*, 905–913. [CrossRef]
52. Hall, M.R.; Najim, K.B. Structural behaviour and durability of steel-reinforced structural Plain/Self-Compacting Rubberised Concrete (PRC/SCRC). *Constr. Build. Mater.* **2014**, *73*, 490–497. [CrossRef]
53. EFNARC. The European Guidelines for Self-Compacting Concrete,. The European Ready-Mix Concrete Organisation EFNARC. 2005. Available online: https://www.theconcreteinitiative.eu/images/ECP_Documents/EuropeanGuidelinesSelfCompactingConcrete.pdf (accessed on 1 May 2023).
54. *EN 12350-8:2019*; Testing Fresh Concrete—Part 8: Self-Compacting Concrete—Slump Flow Test. European Committee for Standardization (CEN): Bruxelles, Belgium, 2010.
55. *EN 12350-10:2010*; Testing Fresh Concrete—Part 10: Self-Compacting Concrete—L Box Test. European Committee for Standardization (CEN): Bruxelles, Belgium, 2010.
56. *EN 12350-12:2010*; Testing Fresh Concrete—Part 11: Self-Compacting Concrete—Sieve Segregation Test. European Committee for Standardization (CEN): Bruxelles, Belgium, 2010.
57. *EN 12350-12:2010*; Testing Fresh Concrete—Part 12: Self-Compacting Concrete—J-Ring Test. European Committee for Standardization (CEN): Bruxelles, Belgium, 2010.
58. *EN 12390-3:2019*; Testing Hardened Concrete—Part 3: Compressive Strength of Test Specimens. European Committee for Standardization (CEN): Bruxelles, Belgium, 2019.
59. *EN 12390-5:2019*; Testing Hardened Concrete—Part 5: Flexural Strength of Test Specimens. European Committee for Standardization (CEN): Bruxelles, Belgium, 2019.
60. *EN 12390-13:2019*; Testing Hardened Concrete—Part 13: Determination of Secant Modulus of Elasticity in Compression. European Committee for Standardization (CEN): Bruxelles, Belgium, 2019.
61. RILEM. RILEM TC 116-PCD: Permeability of Concrete as a Criterion of its Durability—C. Determination of the capillary absorption of water of hardened concrete. *Mater. Struct. Constr.* **1999**, *32*, 174–179.
62. *EN 12390-8:2019*; Testing Hardened Concrete—Part 8: Depth of Penetration of Water under Pressure. European Committee for Standardization (CEN): Bruxelles, Belgium, 2019.
63. *EN 12390-16:2019*; Testing Hardened Concrete. Determination of the Shrinkage of Concrete. European Committee for Standardization (CEN): Bruxelles, Belgium, 2019.
64. *CEN/TS 12390-9:2016*; Testing Hardened Concrete—Part 9: Freeze-Thaw Resistance with De-Icing Salts—Scaling. European Committee for Standardization (CEN): Bruxelles, Belgium, 2016.
65. RILEM. Recommendation of RILEM TC 200-HTC: Mechanical concrete properties at high temperatures—Modelling and applications. *Mater. Struct.* **2007**, *40*, 841–853. [CrossRef]
66. *EN 12667:2001*; Thermal Performance of Building Materials and Products—Determination of Thermal Resistance by Means of Guarded Hot Plate and Heat Flow Meter Methods—Products of High and Medium Thermal Resistance. European Committee for Standardization (CEN): Bruxelles, Belgium, 2001.
67. *ISO 8302:1991*; Thermal Insulation—Determination of Steady-State Thermal Resistance and Related Properties—Guarded Hot Plate Apparatus. ISO—International Organization for Standardization: Geneva, Switzerland, 1991.
68. RILEM. *Performance-Based Specifications and Control of Concrete Durability: State-of-the-Art Report RILEM TC 230-PSC*; Springer: Amsterdam, The Netherlands, 2016. [CrossRef]
69. *HRN 1128:2007*; Concrete—Guidelines for the Implementation of HRN EN 206-1. European Committee for Standardization (CEN): Bruxelles, Belgium, 2007.
70. Bjegović, D.; Štirmer, N. Teorija i Tehnologija Betona, Građevinski Fakultet Zagreb. 2018. Available online: https://www.bib.irb.hr/763135 (accessed on 1 May 2023)
71. *EN 206:2013+A2:2021*; Concrete—Specification, Performance, Production and Conformity. European Committee for Standardization (CEN): Bruxelles, Belgium, 2013.
72. Hernández-Olivares, F.; Barluenga, G. Fire performance of recycled rubber-filled high-strength concrete. *Cem. Concr. Res.* **2004**, *34*, 109–117. [CrossRef]
73. Halstead, P.E.; Moore, A.E. 769. The thermal dissociation of calcium hydroxide. *J. Chem. Soc.* **1957**, 3873–3875. [CrossRef]

74. Nazri, F.M.; Shahidan, S.; Baharuddin, N.K.; Beddu, S.; Bakar, B.H.A. Effects of heating durations on normal concrete residual properties: Compressive strength and mass loss. *IOP Conf. Ser. Mater. Sci. Eng.* **2017**, *271*, 12013. [CrossRef]
75. Kodur, V. Properties of Concrete at Elevated Temperatures. *ISRN Civ. Eng.* **2014**, *2014*, 468510. [CrossRef]
76. Richardson, A.E.; Coventry, K.A.; Ward, G. Freeze/thaw protection of concrete with optimum rubber crumb content. *J. Clean. Prod.* **2012**, *23*, 96–103. [CrossRef]
77. *ASTM C597-16*; Standard Test Method for Pulse Velocity through Concrete, Annual Book of ASTM Standards. ASTM—American Society for Testing and Materials: West Conshohocken, PA, USA, 2009.
78. Topçu, I.B.; Demir, A. Durability of Rubberized Mortar and Concrete. *J. Mater. Civ. Eng.* **2007**, *19*, 173–178. [CrossRef]
79. Strukar, K.; Šipoš, T.K.; Dokšanović, T.; Rodrigues, H. Experimental Study of Rubberized Concrete Stress-Strain Behavior for Improving Constitutive Models. *Materials* **2018**, *11*, 2245. . [CrossRef]
80. *EN 1992-1-2:2004+AC:2008*; Eurocode 2: Design of Concrete Structures—Part 1–2: General Rules—Structural Fire Design. European Committee for Standardization (CEN): Bruxelles, Belgium, 2008.